

1 OCA-B does not act as a transcriptional co-activator in T cells

2 Running title: Extrinsic role for *Pou2af1* in T cells

3

4 Félix Lombard-Vadnais^{1, 2}, Julie Lacombe³, Geneviève Chabot-Roy¹, Mathieu Ferron^{3,4,5}, Sylvie
5 Lesage^{1,6}

6

7 ¹ Immunologie-oncologie, Centre de recherche de l'Hôpital Maisonneuve-Rosemont, Montréal,
8 QC, H1T 2M4, Canada

9 ² Department of Microbiology & Immunology, McGill University, Montreal, QC, H3A 0G4, Canada

10 ³ Maladies cardiovasculaires et métaboliques, Institut de recherches cliniques de Montréal,
11 Montréal, QC, H2W 1R7, Canada

12 ⁴ Département de médecine, Université de Montréal, Montréal, QC, H3T 1J4, Canada

13 ⁵ Department of Experimental Medicine, McGill University, Montreal, QC, H3A 0G4, Canada

14 ⁶ Département de microbiologie, infectiologie et immunologie, Université de Montréal, Montréal,
15 QC, H3T 1J4, Canada

16

17 *Correspondence: Sylvie Lesage, 514-252-3400 ext 4649, sylvie.lesage@umontreal.ca

18

19 Keywords: B cells / OCA-B / *Pou2af1* / T cells / germinal centers/ Tfh

20

21 **Abstract**

22 *Pou2af1* encodes for OCA-B, a coactivator of OCT-1/2 transcription factors, which plays a key
23 role in B cell maturation. The function of OCA-B has also been studied in T cells, where T cells
24 from *Pou2af1*^{-/-} mice have impaired functions, such as cytokine production and T follicular helper
25 (Tfh) differentiation. Arguably, some of these T cell phenotypes may result from impaired T-B
26 interactions, secondary to the well-documented B cell defects in *Pou2af1*^{-/-} mice. Yet, *Pou2af1*
27 is actively transcribed in activated T cells, suggesting a T cell-intrinsic role. To isolate the T cell-
28 intrinsic impact of *Pou2af1*, we generated *Pou2af1*^{fl/fl} mice with specific genetic disruption of
29 *Pou2af1* either in all hematopoietic cells or exclusively in T cells. While we confirm that *Pou2af1*
30 is expressed in activated T cells, we surprisingly find that T cell cytokine production is not
31 impaired in *Pou2af1*-deficient T cells. Moreover, *Pou2af1*-sufficient and -deficient T cells have
32 comparable transcriptome profiles, arguing against a T cell-intrinsic role for *Pou2af1*. In line with
33 these observations, we demonstrate that Tfh maturation is influenced by T cell-extrinsic deletion
34 of *Pou2af1*, as observed both in competitive bone marrow chimeras and in *Pou2af1*^{fl/fl} mice with
35 specific deletion in B cells. Overall, this study provides strong evidence that *Pou2af1* does not
36 act as a transcriptional coactivator in T cells, and conclusively demonstrates that loss of OCA-B
37 in B cells indirectly impacts Tfh differentiation, clarifying the role of OCA-B in the immune system.

38

39 Keywords: B cells / OCA-B / Pou2af1 / T cells / germinal centers/ Tfh

40 INTRODUCTION

41

42 OCA-B (Oct-coactivator from B cells, also known as OBF-1 or BOB.1) is encoded by the *Pou2af1*
43 gene and was first identified in B cell extracts on the basis of its ability to promote
44 immunoglobulin (Ig) gene transcription ¹. It is a transcriptional coactivator that interacts with the
45 ubiquitously expressed OCT-1 and the B cell-specific OCT-2 transcription factors ^{1, 2}. OCA-B
46 expression is restricted to the hematopoietic system, with strong expression in the spleen, lymph
47 nodes (LN), bone marrow and blood ^{2, 3}.

48

49 The first *in vitro* studies of OCA-B function suggested that OCA-B was one of the main drivers
50 of Ig gene transcription in B cells ^{1, 2}. However, the generation of the B6.129S-*Pou2af1*^{-/-} mouse,
51 hereafter referred to as *Pou2af1*^{-/-} mice, in which expression of OCA-B is disrupted in all cell
52 types, revealed that OCA-B is dispensable for Ig transcription ^{4, 5}. *Pou2af1* mRNA is detectable
53 in B cells at all stages of maturation ⁶, and *Pou2af1* deficiency impairs many aspects of B cell
54 biology including B cell development ⁷⁻¹⁰, germinal center (GC) induction ^{4, 5, 11}, IgG production
55 ^{4, 5}, B cell receptor signaling ¹² and plasma cell differentiation ¹³. The target genes of OCA-
56 B/OCT-1/2 complexes remain mostly unknown but candidate genes include *Spib* and *Bcl6* ^{14, 15},
57 both of which contribute to GC B cell differentiation ^{16, 17}, such that this could explain the reduced
58 ability of *Pou2af1*^{-/-} B cells to differentiate into GC B cells.

59

60 In addition to B cells, the function of OCA-B has been studied in T cells. Indeed, *Pou2af1* is
61 transcribed in T cells following *in vitro* activation ^{18, 19}. As OCT-1 is ubiquitously expressed, OCA-
62 B in T cells could act through OCT-1 coactivation. Notably, T follicular helper (Tfh) and T helper

63 17 (Th17) differentiation as well as CD4⁺ T cell cytokine production are impaired in *Pou2af1*^{-/-}
64 mice^{18, 20, 21}. Still, due to the germline disruption of *Pou2af1* in these mice, one cannot conclude
65 whether the T cell phenotypes are due to a cell-intrinsic loss of *Pou2af1* expression or are
66 indirectly attributable to the loss of *Pou2af1* expression in other hematopoietic cells.

67

68 To determine the T cell-intrinsic roles for OCA-B, we generated mouse models in which we
69 performed conditional deletion of *Pou2af1* specifically in hematopoietic cells or in T cells. Using
70 these models, we provide strong evidence that *Pou2af1* does not impact T cell cytokine
71 production or Th17 differentiation, and does not act as a transcriptional coactivator in T cells.
72 Rather, we demonstrate that *Pou2af1* regulates Tfh differentiation in a T cell-extrinsic manner,
73 specifically via *Pou2af1*-expressing B cells.

74 **RESULTS**

75 **Generation of a *Pou2af1^{fl/fl}* mouse for cell-specific *Pou2af1* deletion**

76 In order to generate a mouse strain with cell-specific disruption of the *Pou2af1* gene, we obtained
77 *Pou2af1^{+LacZ}* mice (*Pou2af1^{tm1a(KOMP)Wtsi}*) from the KOMP Repository²². In this mouse strain, the
78 *Pou2af1* locus has been targeted to generate a *knockout-first* allele which can be converted to
79 a conditional (F1, floxed) allele through FLP-mediated recombination (Supplementary figure 1a).
80 Proper targeting of the locus was confirmed through 5' and 3' long range PCR performed on
81 genomic DNA isolated from mouse tails (Supplementary figure 1b). Genotyping PCR using
82 internal primers also confirmed the generation of *Pou2af1^{+LacZ}* mice (Supplementary figure 1c).
83 These animals were next crossed with ACTBFLPe transgenic mice, which expressed the FLPe
84 recombinase gene under the direction of the human ACTB promoter²³, to excise the LacZ and
85 Neomycin (Neo) cassettes. The resulting ACTBFLPe.*Pou2af1^{+fl}* mice were then crossed with
86 C57BL/6J mice to isolate the floxed allele from the ACTBFLPe transgene and proper
87 recombination at the *Pou2af1* locus was confirmed in the progeny of these mice using specific
88 genotyping PCR (Supplementary figure 1d). *Pou2af1^{+fl}* mice were intercrossed to obtain
89 *Pou2af1^{fl/fl}* mice.

90

91 To disrupt the *Pou2af1* gene in all hematopoietic cells, *Pou2af1^{fl/fl}* mice were crossed to Vav-
92 Cre⁺ mice^{24, 25}. Complete absence of *Pou2af1* mRNA expression was confirmed by RT-qPCR
93 on spleen cells from Vav-Cre⁺ and Vav-Cre⁻ littermates (deletion > 99%) (Supplementary figure
94 1e-f). As for *Pou2af1^{-/-}* mice^{4, 7, 20}, B cell proportion and numbers were reduced in the spleen,
95 Peyer's patches (PP) and mesenteric LNs (mLNs) of Vav-Cre⁺.*Pou2af1^{fl/fl}* mice relative to Vav-
96 Cre⁻ littermates (Figure 1a, b). Similar to *Pou2af1^{-/-}* mice²⁰, Vav-Cre⁺.*Pou2af1^{fl/fl}* mice also

97 showed a reduction of GC B cells (GL-7⁺FAS⁺) in both PP and mLNs relative to littermate control
98 mice (Figure 1c, d). In addition, most of the remaining GL-7⁺FAS⁺ GC B cells in Vav-
99 Cre⁺.*Pou2af1*^{fl/fl} mice expressed a CD86⁺CXCR4^{Low} phenotype (Figure 1e, f). The low number
100 of GC B cells in Vav-Cre⁺.*Pou2af1*^{fl/fl} mice are thus skewed towards a phenotype associated with
101 light zone B cells, suggesting that GC B cell differentiation is perturbed in the absence of OCA-
102 B.

103

104 ***Pou2af1* is expressed in T cells**

105 Before investigating the effect of a T cell-specific deletion of *Pou2af1*, we validated that OCA-B
106 was expressed in T cells. With the anti-OCA-B 6F10 monoclonal antibody yielding non-specific
107 binding (Supplementary figure 2a, b), we quantified *Pou2af1* transcription by measuring mRNA
108 levels in *Pou2af1*-sufficient mice. *Pou2af1* mRNA was expectedly abundant in total splenocytes,
109 whereas mRNA levels were barely detectable in T cells (Figure 2a). As previously reported ²⁶,
110 *in vitro* activation of T cells induced a small but significant increase in *Pou2af1* mRNA levels
111 (Figure 2a). These data show that OCA-B is expressed at low levels in total T cells and its
112 expression can be induced upon activation. OCA-B expression was specific, as *Pou2af1* mRNA
113 was undetectable in both unactivated and activated T cells isolated from either Vav-
114 Cre⁺.*Pou2af1*^{fl/fl} or CD4-Cre⁺.*Pou2af1*^{fl/fl} mice (Figure 2a). Note that CD4-Cre is expressed in the
115 early CD4⁺CD8⁺thymic differentiation stage, such that genetic deletion is transmitted to all
116 daughter cells, therefore resulting in targeted gene deletion in both CD4⁺ and CD8⁺ T cells
117 (Supplementary figure 2c, d) ²⁷. As previously reported for *Pou2af1*^{-/-} mice ^{5, 10, 20}, deletion of
118 *Pou2af1* in both Vav-Cre⁺.*Pou2af1*^{fl/fl} and CD4-Cre⁺.*Pou2af1*^{fl/fl} mice did not affect CD4⁺ and
119 CD8⁺ T cell numbers in secondary lymphoid organs (Supplementary figure 2e, f). Taken

120 together, these data show that *Pou2af1* deletion is efficient in both *Vav-Cre⁺.Pou2af1^{fl/fl}* and
121 *CD4-Cre⁺.Pou2af1^{fl/fl}* mice. Indeed, B cell phenotypes in *Vav-Cre⁺.Pou2af1^{fl/fl}* mice recapitulate
122 those observed in *Pou2af1^{-/-}* mice, demonstrating that *Pou2af1* is efficiently deleted in this
123 model. In addition, *Pou2af1* mRNA is undetectable in T cells from both *Vav-Cre⁺.Pou2af1^{fl/fl}* and
124 *CD4-Cre⁺.Pou2af1^{fl/fl}* mice. More importantly, these data confirm that OCA-B is expressed, all
125 be it at low levels, in T cells.

126

127 ***Pou2af1* is dispensable for previously reported T cell phenotypes**

128 We next sought to investigate whether T cell phenotypes previously reported in *Pou2af1^{-/-}* mice
129 were T cell-intrinsic or extrinsic. One of the reported T cell phenotypes in *Pou2af1^{-/-}* mice is
130 impaired cytokine production¹⁸. Specifically, IL-2 cytokine production was quantified in CD4⁺ T
131 cells that had been stimulated with anti-CD3 and anti-CD28 antibodies, rested for 8 days, and
132 restimulated with anti-CD3 and anti-CD28 antibodies for 6 hours. Under these conditions, IL-2
133 cytokine production by CD4⁺ T cells from *Pou2af1^{-/-}* mice was shown to be significantly
134 decreased when compared to B6 mice¹⁸. Here, we quantified IL-2, TNF- α and IFN- γ cytokine
135 production in CD4⁺ T cells from *CD4-Cre⁺.Pou2af1^{fl/fl}* relative to *Cre⁻.Pou2af1^{fl/fl}* littermate
136 controls, using a similar CD4⁺ T cell activation protocol, with an 8 day rest period prior to a 6h
137 restimulation with anti-CD3 and anti-CD28 antibodies. We found that *Pou2af1*-sufficient and -
138 deficient CD4⁺ T cells both produced similar levels of IL-2, TNF- α and IFN- γ (Figure 2b, c),
139 suggesting that *Pou2af1* plays a cell-extrinsic role in facilitating CD4⁺ T cell cytokine production.
140 To validate the cell-extrinsic role of *Pou2af1*, we also assessed IL-2, TNF- α and IFN- γ cytokine
141 production in CD4⁺ T cells from *Vav-Cre⁺.Pou2af1^{fl/fl}* relative to *Cre⁻.Pou2af1^{fl/fl}* littermate
142 controls. In this model, with the deletion of *Pou2af1* in all hematopoietic cells, we expected that

143 CD4⁺ T cell cytokine production would be impaired in *Pou2af1*-deficient T cells, similar to what
144 had been observed in *Pou2af1*^{-/-} mice¹⁸. However, IL-2, TNF- α and IFN- γ cytokine production
145 was similar in CD4⁺ T cells from *Vav-Cre*⁺.*Pou2af1*^{fl/fl} and *Cre*.*Pou2af1*^{fl/fl} mice (Figure 2d). This
146 was observed through a wide range of anti-CD3 concentration, in the presence or absence of
147 co-stimulation (Figure 2e, f). These results thus contrast with previous findings¹⁸ and suggest
148 that *Pou2af1* does not impact CD4⁺ T cell cytokine production neither directly, nor indirectly.

149

150 Due to the discrepancy between the CD4⁺ T cell cytokine production of *Pou2af1*^{-/-} mice and of
151 our newly generated *Pou2af1*^{fl/fl} mice, we considered potential differences in the genetic make-
152 up of the strains. The same exons, namely 2, 3 and 4, are targeted in both models⁵ and
153 Supplementary figure 1). The main difference is genetic background. *Pou2af1* gene targeting in
154 the *Pou2af1*^{-/-} mice was initially performed in 129S embryonic stem cells and the resulting mice
155 were kept on a mixed B6 and 129S genetic background⁵. In contrast, gene targeting in the
156 *Pou2af1*^{fl/fl} mice described here was performed directly on C57BL/6N-A^{tm1Brd} background and
157 *Pou2af1*^{fl/fl} mice were maintained by backcrossing to B6 mice. As the level of CD4⁺ T cell
158 cytokine production from *Pou2af1*^{-/-} mice on a mixed genetic background was compared to that
159 of CD4⁺ T cells from B6 mice¹⁸, we questioned whether genetic variants from the 129S
160 background could explain the difference in phenotype. We quantified IL-2 cytokine production in
161 CD4⁺ T cell from B6 and 129S mice and found that IL-2 production was significantly reduced in
162 CD4⁺ T cell from 129S relative to B6 mice (Figure 2g, h). Next, we acquired *Pou2af1*^{-/-} mice with
163 a mixed genetic background and tested IL-2 production from CD4⁺ T cells. When compared
164 among littermates (i.e. with similar mixed genetic background), IL-2 production was not affected
165 by the *Pou2af1* genotype (Figure 2i). Altogether, these data suggest that genetic variants from

166 the 129S background in *Pou2af1*^{-/-} mice likely affect CD4⁺ T cell cytokine production and that
167 *Pou2af1* expression is dispensable for optimal cytokine production by CD4⁺ T cells.

168

169 The observation that potential 129S carryover genes could affect T cell phenotypes prompted
170 us to revisit the impact of *Pou2af1* on Th17 differentiation²¹ and memory CD4⁺ T cells¹⁸. When
171 subjected to Th17 differentiation conditions, T cells from *Vav-Cre*⁺.*Pou2af1*^{fl/fl} and *Vav-Cre*⁻
172 *.Pou2af1*^{fl/fl} littermates showed similar levels of ROR γ t induction and IL-17 production,
173 demonstrating that Th17 differentiation is not affected by the genetic deletion of *Pou2af1* (Figure
174 **3a-c**). Th17 differentiation and IL-17 production was also similar for CD4⁺ T cells from *Pou2af1*⁻
175 ⁻ mice and the littermate controls (Figure **3d, e**). CD4⁺ T cells with a memory phenotype can be
176 distinguished from naïve cells based on a CD62L^{Lo}CD44^{Hi}CD45RB^{Lo} phenotype. The absence
177 of CD25 expression also discriminates memory CD4⁺ T cells from early effector T cells²⁸. No
178 difference in the percentage or number of CD4⁺ T cells with a memory phenotype was observed
179 in the spleen, bone marrow and LN for both *Vav*- and *CD4-Cre*⁺.*Pou2af1*^{fl/fl} mice relative to their
180 littermate controls (Figure **3f, g** and Supplementary figure 3). Altogether, these results argue
181 against an effect of *Pou2af1* on Th17 differentiation and CD4⁺ T cell memory phenotype.

182

183 **T cell-extrinsic impact of *Pou2af1* deletion on Tfh and GC development**

184 *Pou2af1*^{-/-} mice also display a strong reduction of Tfh in PP at steady state, relative to wild type
185 (WT) mice²⁰. In contrast to the other T cell traits investigated above, we find a clear reduction
186 in the percentage and number of Tfh in both the PP and mLN of *Vav-Cre*⁺.*Pou2af1*^{fl/fl} mice
187 (Figure **4a, b** and Supplementary figure **4a, e**). *Pou2af1* expression in hematopoietic cells is
188 therefore necessary for optimal Tfh differentiation. Interestingly, while Tfh are considerably

189 reduced in *Vav-Cre⁺.Pou2af1^{fl/fl}* mice, early Tfh (CXCR5^{Low}PD-1^{Low}) are present in similar
190 proportions in PP and mLN (Figure 4c and Supplementary figure 4b) and are increased numbers
191 in PP (Supplementary figure 4f), relative to *Cre⁻* littermate controls. When gated on total CD4⁺ T
192 cells expressing CXCR5 and PD-1, to include both early and mature Tfh, we observe a severe
193 decrease in the expression level of CXCR5 and PD-1 (Figure 4d). These data suggest that Tfh
194 differentiation is blocked at the early Tfh maturation stage in *Vav-Cre⁺.Pou2af1^{fl/fl}* mice.

195

196 To determine if *Pou2af1* plays a T cell-intrinsic role in Tfh differentiation, we studied Tfh
197 differentiation in PP and mLN from *CD4-Cre⁺.Pou2af1^{fl/fl}* mice. In contrast to *Pou2af1^{-/-}* mice and
198 *Vav-Cre⁺.Pou2af1^{fl/fl}* mice, the proportion and number of Tfh and of early Tfh was not affected
199 by the specific deletion of *Pou2af1* in T cells from both PP and mLN (Figure 4e-g and
200 Supplementary figure 4a, b, g, h). In addition, specific disruption of *Pou2af1* in T cells did not
201 affect the percentage and number of GC B cells in PP and in mLN (Figure 4h and Supplementary
202 figure 4c, i). The GC B cell bias towards a light zone phenotype observed in the *Vav-*
203 *Cre⁺.Pou2af1^{fl/fl}* mice (Figure 1e, f) was also not observed in *CD4-Cre⁺.Pou2af1^{fl/fl}* mice (Figure
204 4i and Supplementary figure 4d). These results suggest that T cell-intrinsic expression of
205 *Pou2af1* is not necessary for the development of both Tfh and GCs.

206

207 As *Pou2af1* mRNA levels are low in naïve T cells and induced upon activation (Figure 2a), we
208 reasoned that Tfh differentiation in *CD4-Cre⁺.Pou2af1^{fl/fl}* mice may only be impaired upon
209 immunization rather than steady state conditions. To test this possibility, we immunized *Vav-*
210 and *CD4-Cre⁺.Pou2af1^{fl/fl}* mice as well as *Cre⁻.Pou2af1^{fl/fl}* littermate controls with sheep red
211 blood cells, as they induce robust GC formation in the spleen²⁹. Ten days post-immunization,

212 we quantified GC B cells and Tfh in the spleen of these mice. Expectedly, the proportion of PD-
213 1⁺CXCR5⁺ Tfh (Figure 4j, k) and GL-7⁺FAS⁺ GC B cells (Figure 4l) were low in Vav-
214 Cre⁺.*Pou2af1*^{fl/fl} mice. However, both CD4-Cre⁺.*Pou2af1*^{fl/fl} and littermate controls had similar
215 levels of Tfh and GC B cells in the spleens (Figure 4j-l). Consistent with our data in the PPs and
216 mLNs at steady state, we observed a reduction of PD-1 and CXCR5 RFI in Tfh from Vav-
217 Cre⁺.*Pou2af1*^{fl/fl} mice relative to both CD4-Cre⁺.*Pou2af1*^{fl/fl} mice and littermate controls
218 (Supplementary figure 5a). Altogether, these results strongly point to a T cell-extrinsic role of
219 *Pou2af1* in regulating Tfh differentiation in *Pou2af1*^{-/-} mice.

220

221 **OCA-B is not an active transcriptional coactivator in T cells**

222 As we observed no T cell-intrinsic phenotypes in the absence of *Pou2af1*, we sought to
223 investigate whether the increase in *Pou2af1* mRNA in activated T cells has an impact on the T
224 cell transcriptome. OCA-B associates with the OCT-1 and OCT-2 transcription factors to regulate
225 transcription of their target genes^{1,2}. As OCT-1 is expressed in both CD4⁺ and CD8⁺ T cells³⁰,
226 OCA-B may act as a transcriptional cofactor in activated T cells. To identify the potential
227 consequence of *Pou2af1* induction on the T cell transcriptome, we sorted naïve CD4⁺ and CD8⁺
228 T cells from the spleen of CD4-Cre⁻.*Pou2af1*^{fl/fl}, CD4-Cre⁺.*Pou2af1*^{fl/+} and CD4-Cre⁺.*Pou2af1*^{fl/fl}
229 littermates. Sorted cells were stimulated *in vitro* with anti-CD3 and anti-CD28 for 48h hours, RNA
230 was isolated and subjected to RNA-Seq analysis. Principal component analysis (PCA) applied
231 to the 500 most differentially expressed genes did not segregate T cells on the basis of their
232 genotype (Figure 5a), suggesting an absence of transcriptomic regulation by *Pou2af1*. *Pou2af1*
233 mRNA expression was significantly decreased in T cells from CD4-Cre⁺.*Pou2af1*^{fl/fl} mice relative
234 to T cells from CD4-Cre⁻.*Pou2af1*^{fl/fl} mice, confirming that *Pou2af1* mRNA is expressed in

235 activated CD4⁺ and CD8⁺ T cells (Figure 5b and Supplementary figure 6a). Apart from *Pou2af1*,
236 only four genes were significantly differentially expressed when comparing CD4⁺ or CD8⁺ cells
237 from CD4-Cre⁻.*Pou2af1*^{fl/fl} and CD4-Cre⁺.*Pou2af1*^{fl/fl} littermates (Figure 5b and Supplementary
238 figure 6a). Among those four genes, only two were observed in both CD4⁺ and CD8⁺ T cells:
239 *Rps3a1* and *Tpm3-rs7*. Of note, these two genes were also differentially expressed in T cells
240 from CD4-Cre⁺.*Pou2af1*^{fl/+} heterozygous mice when compared to CD4-Cre⁻.*Pou2af1*^{fl/fl} mice
241 (Figure 5b), suggesting that the expression of the CD4-Cre transgene may be responsible for
242 these differences, rather than an effect of the *Pou2af1* deletion. Together, these data
243 demonstrate that, although *Pou2af1* is expressed in T cells following *in vitro* stimulation, it does
244 not act as an important coactivator of transcription.

245

246 ***Pou2af1* expression in B cells is necessary for adequate Tfh maturation**

247 Notwithstanding the absence of a T cell-intrinsic role for *Pou2af1*, our data point to a T cell-
248 extrinsic role in Tfh differentiation. To specifically test if the Tfh maturation block observed in
249 *Vav-Cre*⁺.*Pou2af1*^{fl/fl} mice is caused by defective crosstalk between T cells and *Pou2af1*^{-/-}
250 hematopoietic cells *in vivo*, we generated competitive bone marrow chimeras. B6.SJL (CD45.1)
251 and *Vav-Cre*⁺.*Pou2af1*^{fl/fl} (CD45.2) bone marrow were mixed at 1:1 ratio and injected in lethally
252 irradiated B6 x B6.SJL F1 (CD45.1 and CD45.2 co-dominant expression) (Supplementary figure
253 6b). Expectedly, WT B cells (CD45.1) showed a growth advantage over *Pou2af1*-deficient B
254 cells differentiated from *Vav-Cre*⁺.*Pou2af1*^{fl/fl} (CD45.2) bone marrow (Figure 5c, d). In contrast,
255 and consistent with our observations in both *Vav*- and CD4-Cre⁺.*Pou2af1*^{fl/fl} mice
256 (Supplementary figure 2e, f), T cells from WT and *Vav-Cre*⁺.*Pou2af1*^{fl/fl} precursors were present
257 in equal proportions (Figure 5c, d), confirming an absence of competitive disadvantage for

258 *Pou2af1* targeted T cells. We also observed a severe reduction of GC B cells of Vav-
259 *Cre⁺.Pou2af1^{fl/fl}* origin (Supplementary figure 6c, d), confirming the B cell-intrinsic defect of GC
260 induction in the absence of *Pou2af1*. As opposed to the observations made in Vav-
261 *Cre⁺.Pou2af1^{fl/fl}* mice, CD4⁺ T cells were able to fully mature into Tfh in the spleen, PP and mLN
262 of the chimeras, regardless of their genotype (Figure 5e, f). This is likely due to the presence of
263 a sufficient number of OCA-B expressing B cells in this competitive bone marrow chimera setting
264 (Figure 5c), suggesting a T cell extrinsic role for OCA-B in Tfh differentiation. These results are
265 consistent with a previous report also demonstrating a T cell-extrinsic role for OCA-B in Tfh
266 development and function using mixed bone marrow chimeras ³¹.

267

268 Next, to determine if loss of OCA-B in B cells is sufficient to impede Tfh differentiation, we
269 crossed *Pou2af1^{fl/fl}* mice to CD19-Cre⁺ mice to disrupt *Pou2af1* specifically in B cells. The
270 percentage of B cells were reduced in the lymphoid organs of CD19-Cre⁺.*Pou2af1^{fl/fl}* mice, in
271 line with effective *Pou2af1* disruption (Figure 5g). Compared to CD19-Cre⁻ littermates, CD19-
272 Cre⁺.*Pou2af1^{fl/fl}* mice showed a significant reduction in Tfh and a reduced expression of CXCR5
273 and PD-1 on CD4⁺ T cells from the PP and mLN (Figure 5h-j). These results show that specific
274 loss of OCA-B expression in B cells is sufficient to impair Tfh differentiation. Altogether, our data
275 conclusively demonstrate that *Pou2af1* plays a T cell-extrinsic role in Tfh differentiation.

276

277 **DISCUSSION**

278 The levels of expression of *Pou2af1* are clearly more prominent in B cells than in T cells. The
279 Immunological Genome Project database shows that *Pou2af1* mRNA is detectable in all B cell
280 stages, from B cell precursors to plasma cells⁶. Multiple transcriptomic and proteomic databases
281 also show that, among immune cell types, *Pou2af1* expression is undetectable in non-B cells, in
282 both mice and humans^{3, 6, 32}. Still, we and others report that *Pou2af1* expression can be induced
283 in T cells^{19, 26}(and this manuscript), and the biological impact of *Pou2af1* in T cells has been
284 investigated for more than two decades^{19, 33}. By generating a new mouse strain in which
285 *Pou2af1* can be conditionally deleted, we provide evidence that, as opposed to previous reports
286^{18, 21, 34}, *Pou2af1* is dispensable for CD4⁺ T cell cytokine production, Th17 differentiation and
287 does not affect the T cell pool. Using an unbiased approach to determine the impact of *Pou2af1*
288 in regulating the transcriptional profile of CD4⁺ and CD8⁺ T cells, we find that *Pou2af1* does not
289 act as an effective transcriptional coactivator in activated T cells. We also report that *Pou2af1*
290 indirectly promotes the differentiation of CD4⁺ T cells into mature Tfh, via *Pou2af1*-expressing B
291 cells.

292
293 As mentioned, CD4⁺ T cells isolated from B6.129S-*Pou2af1*^{-/-} show defects in cytokine
294 production, immunological memory as well as in Th17 and Tfh differentiation^{18, 20, 21}. Moreover,
295 *Pou2af1* mRNA is induced in activated T cells^{18, 19}. With this growing literature on the role of
296 OCA-B in T cells, we expected to find that T cell specific deletion of *Pou2af1* expression would
297 alter T cell functions. With the two mouse models that specifically target deletion in either all
298 hematopoietic cells or in all T cells, we set out to determine the T cell specific role of OCA-B in
299 transcriptional regulation. Instead, we were taken aback and noted that T cell specific deletion

300 of *Pou2af1* expression does not influence T cell phenotypes and does not significantly affect the
301 T cell transcriptome. We provide evidence to suggest that the difference between our results
302 and that of others appear to stem from the differences in genetic background; whereas our floxed
303 model was generated on the C57BL/6N-A^{tm1Brd} background, the B6.129S-*Pou2af1*^{-/-} model is
304 held on a mixed B6 and 129S genetic background. Notably, we find that cytokine production in
305 T cells from 129S mice is reduced relative to that of B6 mice. These observations are in line with
306 previous reports demonstrating that carryover genes influence the phenotype of knock-out and
307 congenic mice ^{35, 36}.

308

309 Notwithstanding the lack of impact of *Pou2af1* in various T cell phenotypes, hematopoietic
310 deletion of *Pou2af1* expression resulted in a significant decrease in Tfh. Characterization of
311 mature Tfh in CD4-Cre⁺.*Pou2af1*^{fl/fl} mice and in competitive bone marrow experiments confirmed
312 a T cell-extrinsic role of *Pou2af1* in Tfh differentiation. Notably, the proportion and absolute
313 numbers of early Tfh cells were unaffected in Vav-Cre⁺.*Pou2af1*^{fl/fl} mice whereas late Tfh were
314 significantly reduced, suggesting that lack of OCA-B predominantly affects the transition from
315 early Tfh to late Tfh. This is not surprising considering that early Tfh differentiation is highly
316 dependent on DCs ³⁷, which do not express *Pou2af1*. IL-6 and IL-21 produced by DCs during
317 priming of CD4⁺ T cells induce changes in chemokine receptors expression, resulting in
318 migration of early Tfh to the B cell follicle border ³⁸. At this step, early Tfh express low levels of
319 BCL6, CXCR5 and PD-1 and require additional signals to further differentiate into mature Tfh ³⁹.
320 At the T-B border, B cells provide crucial signals to developing Tfh, such as ICOS-L, antigens,
321 and cytokines ^{38, 40}. As B cells express high levels of OCA-B, *Pou2af1* disruption strongly affects
322 their differentiation and functions ^{7, 8, 11}(and this manuscript). The reduction of total B cells and

323 GC B cells in *Pou2af1*^{-/-} and *Vav-Cre*⁺.*Pou2af1*^{fl/fl} mice likely impairs crosstalk between B cells
324 and early Tfh, thereby limiting early Tfh maturation. Using CD19-Cre mice to specifically disrupt
325 *Pou2af1* in B cells, we show that crosstalk between B cells and early Tfh requires OCA-B
326 expression in B cells to promote efficient Tfh maturation. This crosstalk might be impaired in
327 OCA-B-deficient mice through reduced expression of ICOSL, highly expressed by GC B cells ⁴¹,
328 or by impaired cytokine production by B cells. Indeed, OCA-B promotes IL-6 production in
329 activated B cells during infection, and B cell-derived IL-6 can induce Tfh development ³¹.
330 CXCR5⁺PD-1⁺ CD4⁺ T cells from *Pou2af1*^{-/-} mice also display lower BCL6 levels relative to B6
331 mice ²⁰. As such, it was suggested that *Pou2af1* directly promotes Tfh differentiation by
332 regulating BCL6 ²⁰. However, considering that *Pou2af1* indirectly regulates Tfh differentiation,
333 the reduction of BCL6 expression in Tfh from *Pou2af1*^{-/-} mice is most likely caused by the
334 maturation block at the early Tfh stage, which express lower BCL6 levels than mature Tfh ³⁹.
335
336 It is interesting to note that *Pou2af1*^{-/-} mice show a severe reduction in serum IgG, IgA and IgE,
337 while IgM is not affected ^{4, 5, 10}. This feature of the *Pou2af1*^{-/-} mouse does not seem to be
338 attributed to a B cell-intrinsic class switching defect, as *Pou2af1*^{-/-} B cells are able to class switch
339 *in vitro* as efficiently as WT B cells ⁵. Since Tfh directly promote B cell class switching from IgM
340 to other isotypes ^{42, 43}, the lack of mature Tfh indirectly caused by *Pou2af1* deletion in B cells
341 may explain the reduction of IgG, IgA and IgE in the *Pou2af1*^{-/-} mouse. Alternatively, a B cell-
342 intrinsic role of OCA-B in plasma cell differentiation may also contribute to the reduction of
343 isotype switched serum antibody levels ¹³.

344

345 Although *Pou2af1* expression is induced in T cells following activation, we did not identify any T
346 cell intrinsic function. By comparing the mRNA transcriptome of activated T cells isolated from
347 CD4-Cre⁻.*Pou2af1*^{fl/fl} and CD4-Cre⁺.*Pou2af1*^{fl/fl} mice, we further show that OCA-B does not seem
348 to exhibit significant transcriptional activity in T cells. The functional impact, if any, of the low
349 *Pou2af1* mRNA expression levels in activated T cells remains to be determined.

350

351 In conclusion, this study shows that *Pou2af1* is dispensable for most of the T cell-associated
352 phenotypes previously identified in the *Pou2af1*^{-/-} mouse, with the exception of the T cell-extrinsic
353 effect on Tfh differentiation; *Pou2af1* expression in B cells promotes maturation of early Tfh into
354 Tfh *in vivo*. Overall, this study clarifies the role of OCA-B in the immune system, by conclusively
355 demonstrating that *Pou2af1* does not act as a coactivator of transcription in T cells, and therefore
356 does not bear T cell-intrinsic activities. Furthermore, we demonstrate that OCA-B expression in
357 B cells facilitates Tfh differentiation, explaining the T cell-extrinsic role of *Pou2af1*.

358

359 **METHODS**

360 **Mice**

361 B6 mice (#000664, Jax labs, Bar Harbor, United States) were crossed to B6.SJL mice (#002014,
362 Jax labs) to generate F1 mice (B6.1.2), with co-dominant expression of CD45.1 and CD45.2 on
363 all hematopoietic cells, were used as bone marrow chimera recipients. *Pou2af1^{+LacZ}* mice
364 (*Pou2af1^{tm1a(KOMP)Wtsi}*) were obtained from the KOMP Repository (#049152-UCD, Davis, United
365 States) ²², for which embryonic stem cells were of C57BL/6N-A^{tm1Brd} background. Proper
366 targeting of the locus was confirmed by 5' and 3' long range PCR performed on genomic DNA
367 isolated from mouse tails using a combination of two primers located respectively inside and
368 outside the targeting construct. Genotyping PCR using internal primers also confirmed the
369 generation of *Pou2af1^{+LacZ}* mice. The genotyping primers are: P1, 5'-
370 TACAGAGAGACTAGACACGGTCTGC-3'; P2, 5'-AGAAGGCCTCGTTACACTCCTATGC-3';
371 P3, 5'-GAGATGGCGCAACGCAATTAATG-3'; P4, 5'-GATGAGGACTCTGGGTTTCAGAGAGG-
372 3'; P5, 5'-GGGATCTCATGCTGGAGTTCTTCG-3'. These mice were crossed with ACTBFLPe
373 Tg mice (#005703, Jax labs) to excise the LacZ and Neo cassettes and generate *Pou2af1^{+fl}*
374 mice (*Pou2af1^{tm1c}*; see Supplementary figure 1) in which exon 2, 3 and 4 are flanked by loxP
375 sites. The ACTBFLPe transgene was removed by subsequent breeding to B6 mice. *Pou2af1^{+fl}*
376 mice were intercrossed to generate *Pou2af1^{fl/fl}* mice. *Vav-Cre⁺.Pou2af1^{fl/fl}*, *CD4-Cre⁺.Pou2af1^{fl/fl}*
377 and *CD19-Cre⁺.Pou2af1^{fl/fl}* mice (#008610 and #022071, #006785, Jax labs) were generated by
378 crossing *Cre⁺.Pou2af1^{fl/+}* mice to *Pou2af1^{fl/fl}*, to avoid germline deletion ⁴⁴. ROSA-YFP mice
379 (#007903, Jax labs) were crossed to *CD4-Cre⁺* mice to validate genetic deletion in T cells. 129S
380 and *Pou2af1^{-/-}* mice (#002448, #007596, Jax labs) were used to test the influence of the genetic
381 background on the phenotypes. Genotype of all transgenic mice was verified by PCR.

382 Transgenic positive and negative littermates were used in every experiment. Male and female
383 mice were used in this study and no phenotypic difference was observed based on sex. All of
384 the mouse strains were maintained at the Maisonneuve-Rosemont Hospital animal facility
385 (Montreal, Canada). The Maisonneuve-Rosemont Hospital ethics committee, overseen by the
386 Canadian Council for Animal Protection, approved the experimental procedures.

387

388 **Generation of bone marrow chimeras**

389 Prior to irradiation, recipient mice were injected intraperitoneally with 1 mL of PBS to avoid
390 dehydration. Bone marrow cell suspensions were prepared from the tibia and femur of 10-week-
391 old mice in sterile RPMI. The red blood cells were lysed using NH_4Cl and the bone marrow single
392 cell suspension were prepared in sterile PBS. A 1:1 bone marrow ratio was confirmed by flow
393 cytometry (with anti-CD45.1 and anti-CD45.2 antibodies) prior to injection. Eight-week-old
394 recipient mice were irradiated at 11Gy, using linac X-ray source and, subsequently, injected
395 intravenously with 2×10^6 bone marrow cells.

396

397 **Sheep red blood cell immunization**

398 Mice were injected intra-peritoneally with 5×10^8 sheep red blood cells (Innovative Research,
399 Novi, United States) diluted in PBS. Ten days after injection, the spleens were collected for flow
400 cytometry analysis.

401

402 **Flow cytometry and cell sorting**

403 Spleen, bone marrow, PP and LNs were pressed through a 70- μm cell strainer (Thermo Fisher
404 Scientific, Waltham, United States). Spleen cell suspensions were treated with NH_4Cl to lyse red

405 blood cells. Single-cell suspensions were stained for 30 minutes at 4°C with different
406 combinations of antibodies listed as target (clone): From BioLegend (San Diego, United States),
407 B220 (RA3-6B2), CD4 (GK1.5), CD8a (53-6.7), CD19 (6D5), CD25 (PC61.5.3), CD44 (IM7),
408 CD45.1 (A20), CD45.2 (104), CD45RB (C363-16A), CD62L (MEL-14), CD69 (H1.2F3), CD86
409 (GL-1), CXCR4 (L276F12), CXCR5 (L138D7), GL-7 (GL7), IFN- γ (XMG1.2), IL-2 (JES6-5H4),
410 PD-1 (RMP1-30), TCR β (H57-597), TNF- α (MP6-XT22); From BD Biosciences (New Jersey,
411 United States), CD95 (Jo2); From Thermo Fisher, CD8b (H35-17.2), FoxP3 (FJK-16s), IL-17
412 (eBio1787), ROR γ t (B2D); From Santa Cruz Biotechnology (Dallas, United States), OCA-B
413 (6F10). Biotin-labelled antibodies were revealed with fluorescently-coupled streptavidins from
414 BioLegend. Viable cells were stained using LIVE/DEAD™ Fixable Yellow Dead Cell Stain Kit
415 (Thermo Fisher). Before staining with 6F10 antibodies, cells were fixed and permeabilized using
416 BD Cytotfix/Cytoperm™ kit, as published ¹⁸. Cells were stained in 100 μ l of buffer plus 7.5 μ l of
417 PE-conjugated 6F10 antibodies ¹⁸. For transcription factor staining, cells were treated with
418 FOXP3 Transcription Factor Staining Buffer Set (Thermo Fischer). Data were collected on an
419 LSRFortessaX20 (BD Biosciences), and analyzed with FlowJo software (BD Biosciences). For
420 cell sorting, spleen cell suspensions were stained with antibodies against TCR β and B220, in
421 sterile conditions. T cells were sorted on a FACS Aria II (BD Biosciences) as TCR β ⁺B220⁻ single
422 cells (purity > 99%).

423

424 ***In vitro* T cell stimulation**

425 As described in Shakya *et al.*¹⁸, *in vitro* T cell stimulation was performed in flat bottom 96 well
426 plates (Sarstedt, Nümbrecht, Germany) coated with anti-CD3 (either 1 μ g mL⁻¹ or graded
427 concentrations as indicated, 145-2C11) and anti-CD28 (10 μ g mL⁻¹, 37.51) antibodies in PBS

428 overnight at 4°C. Plates were washed in serum-containing media prior to adding the cells. For
429 primary stimulation, spleen cells ($5 \times 10^5 \text{ mL}^{-1}$) were stimulated for 2 days in complete RPMI-1640
430 medium. In some experiments, cells were analyzed after primary stimulation. Otherwise, cells
431 were rested for 8 days, in complete RPMI-1640 medium with IL-2 (30 U mL^{-1}). For secondary
432 stimulation, rested cells were activated for 6 hours with plate bound anti-CD3 and anti-CD28
433 antibodies, at 1 and $10 \mu\text{g mL}^{-1}$ respectively, in the presence of Brefeldin A ($10 \mu\text{g mL}^{-1}$). Cells
434 were then harvested and stained with antibodies prior to analysis by flow cytometry.

435

436 **RT-qPCR**

437 $5 \cdot 10^6$ sorted T cells were stored in Trizol while the remaining T cells ($2.5 \cdot 10^5$) were
438 activated *in vitro* for 2 days using anti-CD3 and anti-CD28 antibodies. RNA extraction for all
439 samples was conducted as indicated by the manufacturer (Trizol, Thermo Fisher Scientific).
440 Mouse *Pou2af1* mRNA levels were measured using primers targeting exons 4 and 5 of *Pou2af1*
441 (*Pou2af1*-F: 5'-CCTGCCTTGACATGGAGGTT-3' and *Pou2af1*-R: 5'-
442 AGTGCTTCTTGGCGTGACAT-3'), *Gapdh* (*Gapdh*-F:5'-TCAACGGCACAGTCAAGG-3' and
443 *Gapdh*-R: 5'-ACTCCACGACATACTCAGC-3') and *Actb* (*Actb*-F:5'-
444 GAAATCGTGCGTGACATCAAAG-3' and *Actb*-R: 5'-TGTAGTTTCATGGATGCCACAG-3')
445 mRNA levels were used as loading controls and ddCT variations calculated in all cases.

446

447 **Th17 differentiation**

448 To differentiate T cells into either Th0 or Th17 profiles, LN cells were activated with plate bound
449 anti-CD3 ($2 \mu\text{g mL}^{-1}$) and anti-CD28 ($2 \mu\text{g mL}^{-1}$) antibodies. While Th0 differentiation proceeded
450 in the absence of cytokines, Th17 was induced in the presence of 2 ng mL^{-1} rhTGF- β 1 and 25

451 ng mL⁻¹ rmlL-6 (both cytokines from Miltenyi Biotec, Bergisch Gladbach, Germany), as described
452 in Yosef *et al.* ²¹. Cells were cultured for 3 days prior to analysis. T cell supernatants were
453 collected at the end of the 3-day culture. Quantification of IL-17A in the media was performed
454 by ELISA as indicated by the manufacturer (Mouse Il-17 Quantikine ELISA Kit, R&D Systems,
455 Minneapolis, United States). For quantifying IL-2 and IL-17A production by flow cytometry, cells
456 were incubated with phorbol 12-myristate 13-acetate (50 ng mL⁻¹), ionomycin (500 ng mL⁻¹) and
457 Brefeldin A (10 µg mL⁻¹) for 4h prior to staining.

458

459 **RNA sequencing**

460 Naïve CD4⁺ and CD8⁺ T cells were sorted from the spleen as CD19-TCR_β⁺CD4⁺CD62L⁺ and
461 CD19-TCR_β⁺CD8⁺CD62L⁺ single cells, respectively (purity > 96%). T cells were activated *in vitro*
462 for two days using anti-CD3 and anti-CD28 antibodies. RNA was isolated using Trizol and sent
463 to the IRIC genomic platform for processing. Libraries were prepared using the KAPA mRNA
464 stranded Hyperprep Kit. Libraries were sequenced using the Illumina NextSeq 500 FASTQ files
465 were trimmed for sequencing adapters and low quality 3' bases using Trimmomatic version 0.35
466 ⁴⁵ and aligned to the reference mouse genome version GRCm38 (gene annotation from
467 Gencode version M25, based on Ensembl 100) using STAR version 2.7.1a ⁴⁶. Read counts were
468 extracted directly from STAR at the gene level. DESeq2 (R; version 1.26) was then used to
469 normalize gene read counts. Batch correction was added to the statistical model for differential
470 expression to adjust for samples sorted on 2 separate days. Log normalized counts were batch
471 corrected using the removeBatchEffect function from the limma R package (v 3.42.2) ⁴⁷ and
472 used as input for PCA and heatmap visualizations. The raw RNAseq data files have been
473 uploaded into the GEO database (accession number: GSE171544).

474 **Statistical analyses**

475 Data were tested for significance using a nonparametric Mann-Whitney *U*-test or a one-way
476 ANOVA, where appropriate. Numbers of animal used per group are indicated in the figure
477 legends. The minimal significance threshold was set at 0.05 for all tests.

478

479 **Acknowledgments:** We thank Dr Frédéric Picard, Dr Heather Melichar and Dr Nathalie
480 Labrecque for a critical review of the manuscript and all laboratory members for helpful
481 discussions. We are grateful for Martine Dupuis from the flow cytometry facility as well as all
482 animal house staff for technical support. We also thank Dr Patrick Gendron from the IRIC
483 platform, and Dr Adam-Nicolas Pelletier from RPM Bioinfo Solutions for expert bioinformatics
484 analyses.

485 **Funding:** This work was supported by a grant from the Natural Sciences and Engineering
486 Research Council of Canada (2019-05047). F.L.-V. hold scholarships from the Fondation de
487 l'Hôpital Maisonneuve-Rosemont, the Cole Foundation, and the Fonds de Recherche Quebec
488 Santé. MF holds a Canada Research Chair in Bone and Energy Metabolism. S.L. is a Research
489 Scholars Emeritus awardee from the Fonds de Recherche Quebec Santé.

490 **Conflict of interest:** The authors declare that they have no conflicts of interest.

491 **Data availability:** The raw RNAseq data files have been uploaded into the GEO database
492 (accession number: GSE171544).

493 **Author contributions:** F.L.-V. designed and conducted most of the experiments, prepared the
494 figures, and wrote the manuscript. J.L. generated and validated the *Pou2af1^{fl/fl}* mouse and
495 designed *Pou2af1* RT-qPCR primers. G.C.-R. performed the flow cytometry analysis of CD4-
496 Cre⁺.ROSA-YFP⁺ mice. M.F. contributed to the generation of the *Pou2af1^{fl/fl}* mouse and to
497 revisions of the manuscript. S.L. supervised the study, wrote and revised the manuscript.

498 **References**

- 499 1. Luo Y, Fujii H, Gerster T, Roeder RG. A novel B cell-derived coactivator potentiates the
500 activation of immunoglobulin promoters by octamer-binding transcription factors. *Cell* 1992;
501 **71**: 231-241.
- 502 2. Strubin M, Newell JW, Matthias P. OBF-1, a novel B cell-specific coactivator that stimulates
503 immunoglobulin promoter activity through association with octamer-binding proteins. *Cell*
504 1995; **80**: 497-506.
- 505 3. Uhlen M, Fagerberg L, Hallstrom BM, *et al.* Proteomics. Tissue-based map of the human
506 proteome. *Science* 2015; **347**: 1260419.
- 507 4. Schubart DB, Rolink A, Kosco-Vilbois MH, Botteri F, Matthias P. B-cell-specific coactivator OBF-
508 1/OCA-B/Bob1 required for immune response and germinal centre formation. *Nature* 1996;
509 **383**: 538-542.
- 510 5. Kim U, Qin XF, Gong S, *et al.* The B-cell-specific transcription coactivator OCA-B/OBF-1/Bob-1 is
511 essential for normal production of immunoglobulin isotypes. *Nature* 1996; **383**: 542-547.
- 512 6. Heng TS, Painter MW, Immunological Genome Project C. The Immunological Genome Project:
513 networks of gene expression in immune cells. *Nat Immunol* 2008; **9**: 1091-1094.
- 514 7. Hess J, Nielsen PJ, Fischer KD, Bujard H, Wirth T. The B lymphocyte-specific coactivator
515 BOB.1/OBF.1 is required at multiple stages of B-cell development. *Mol Cell Biol* 2001; **21**: 1531-
516 1539.
- 517 8. Teitell MA. OCA-B regulation of B-cell development and function. *Trends Immunol* 2003; **24**:
518 546-553.
- 519 9. Samardzic T, Marinkovic D, Nielsen PJ, Nitschke L, Wirth T. BOB.1/OBF.1 deficiency affects
520 marginal-zone B-cell compartment. *Mol Cell Biol* 2002; **22**: 8320-8331.
- 521 10. Nielsen PJ, Georgiev O, Lorenz B, Schaffner W. B lymphocytes are impaired in mice lacking the
522 transcriptional co-activator Bob1/OCA-B/OBF1. *Eur J Immunol* 1996; **26**: 3214-3218.
- 523 11. Qin XF, Reichlin A, Luo Y, Roeder RG, Nussenzweig MC. OCA-B integrates B cell antigen
524 receptor-, CD40L- and IL 4-mediated signals for the germinal center pathway of B cell
525 development. *EMBO J* 1998; **17**: 5066-5075.
- 526 12. Siegel R, Kim U, Patke A, *et al.* Nontranscriptional regulation of SYK by the coactivator OCA-B is
527 required at multiple stages of B cell development. *Cell* 2006; **125**: 761-774.
- 528 13. Corcoran LM, Hasbold J, Dietrich W, *et al.* Differential requirement for OBF-1 during antibody-
529 secreting cell differentiation. *J Exp Med* 2005; **201**: 1385-1396.
- 530 14. Bartholdy B, Du Roure C, Bordon A, Emslie D, Corcoran LM, Matthias P. The Ets factor Spi-B is a
531 direct critical target of the coactivator OBF-1. *Proc Natl Acad Sci U S A* 2006; **103**: 11665-11670.
- 532 15. Chu CS, Hellmuth JC, Singh R, *et al.* Unique Immune Cell Coactivators Specify Locus Control
533 Region Function and Cell Stage. *Mol Cell* 2020; **80**: 845-861 e810.
- 534 16. Su GH, Chen HM, Muthusamy N, *et al.* Defective B cell receptor-mediated responses in mice
535 lacking the Ets protein, Spi-B. *EMBO J* 1997; **16**: 7118-7129.
- 536 17. Basso K, Dalla-Favera R. BCL6: master regulator of the germinal center reaction and key
537 oncogene in B cell lymphomagenesis. *Adv Immunol* 2010; **105**: 193-210.
- 538 18. Shakya A, Goren A, Shalek A, *et al.* Oct1 and OCA-B are selectively required for CD4 memory T
539 cell function. *J Exp Med* 2015; **212**: 2115-2131.

- 540 19. Sauter P, Matthias P. The B cell-specific coactivator OBF-1 (OCA-B, Bob-1) is inducible in T cells
541 and its expression is dispensable for IL-2 gene induction. *Immunobiology* 1997; **198**: 207-216.
- 542 20. Stauss D, Brunner C, Berberich-Siebelt F, Hopken UE, Lipp M, Muller G. The transcriptional
543 coactivator Bob1 promotes the development of follicular T helper cells via Bcl6. *EMBO J* 2016;
544 **35**: 881-898.
- 545 21. Yosef N, Shalek AK, Gaublomme JT, *et al.* Dynamic regulatory network controlling TH17 cell
546 differentiation. *Nature* 2013; **496**: 461-468.
- 547 22. Skarnes WC, Rosen B, West AP, *et al.* A conditional knockout resource for the genome-wide
548 study of mouse gene function. *Nature* 2011; **474**: 337-342.
- 549 23. Rodriguez CI, Buchholz F, Galloway J, *et al.* High-efficiency deleter mice show that FLPe is an
550 alternative to Cre-loxP. *Nat Genet* 2000; **25**: 139-140.
- 551 24. Ogilvy S, Metcalf D, Gibson L, Bath ML, Harris AW, Adams JM. Promoter elements of vav drive
552 transgene expression in vivo throughout the hematopoietic compartment. *Blood* 1999; **94**:
553 1855-1863.
- 554 25. Georgiades P, Ogilvy S, Duval H, *et al.* VavCre transgenic mice: a tool for mutagenesis in
555 hematopoietic and endothelial lineages. *Genesis* 2002; **34**: 251-256.
- 556 26. Mueller K, Quandt J, Marienfeld RB, *et al.* Octamer-dependent transcription in T cells is
557 mediated by NFAT and NF- κ B. *Nucleic Acids Res* 2013; **41**: 2138-2154.
- 558 27. Wolfer A, Bakker T, Wilson A, *et al.* Inactivation of Notch 1 in immature thymocytes does not
559 perturb CD4 or CD8T cell development. *Nat Immunol* 2001; **2**: 235-241.
- 560 28. Moulton VR, Bushar ND, Leeser DB, Patke DS, Farber DL. Divergent generation of
561 heterogeneous memory CD4 T cells. *J Immunol* 2006; **177**: 869-876.
- 562 29. McAllister EJ, Apgar JR, Leung CR, Rickert RC, Jellusova J. New Methods To Analyze B Cell
563 Immune Responses to Thymus-Dependent Antigen Sheep Red Blood Cells. *J Immunol* 2017;
564 **199**: 2998-3003.
- 565 30. Hwang SS, Kim LK, Lee GR, Flavell RA. Role of OCT-1 and partner proteins in T cell
566 differentiation. *Biochim Biophys Acta* 2016; **1859**: 825-831.
- 567 31. Karnowski A, Chevrier S, Belz GT, *et al.* B and T cells collaborate in antiviral responses via IL-6,
568 IL-21, and transcriptional activator and coactivator, Oct2 and OBF-1. *J Exp Med* 2012; **209**:
569 2049-2064.
- 570 32. Schaum N, Karkanas J, Neff NF, *et al.* Single-cell transcriptomics of 20 mouse organs creates a
571 Tabula Muris. *Nature* 2018; **562**: 367-372.
- 572 33. Zwilling S, Dieckmann A, Pfisterer P, Angel P, Wirth T. Inducible expression and phosphorylation
573 of coactivator BOB.1/OBF.1 in T cells. *Science* 1997; **277**: 221-225.
- 574 34. Brunner C, Sindrilaru A, Girkontaite I, Fischer KD, Sunderkotter C, Wirth T. BOB.1/OBF.1 controls
575 the balance of TH1 and TH2 immune responses. *EMBO J* 2007; **26**: 3191-3202.
- 576 35. Hogenbirk MA, Heideman MR, Velds A, *et al.* Differential programming of B cells in AID deficient
577 mice. *PLoS One* 2013; **8**: e69815.
- 578 36. Chisolm DA, Cheng W, Colburn SA, *et al.* Defining Genetic Variation in Widely Used Congenic
579 and Backcrossed Mouse Models Reveals Varied Regulation of Genes Important for Immune
580 Responses. *Immunity* 2019; **51**: 155-168 e155.
- 581 37. Goenka R, Barnett LG, Silver JS, *et al.* Cutting edge: dendritic cell-restricted antigen
582 presentation initiates the follicular helper T cell program but cannot complete ultimate effector
583 differentiation. *J Immunol* 2011; **187**: 1091-1095.

- 584 38. Crotty S. T follicular helper cell differentiation, function, and roles in disease. *Immunity* 2014;
585 **41**: 529-542.
- 586 39. Trub M, Barr TA, Morrison VL, *et al.* Heterogeneity of Phenotype and Function Reflects the
587 Multistage Development of T Follicular Helper Cells. *Front Immunol* 2017; **8**: 489.
- 588 40. Weinstein JS, Bertino SA, Hernandez SG, *et al.* B cells in T follicular helper cell development and
589 function: separable roles in delivery of ICOS ligand and antigen. *J Immunol* 2014; **192**: 3166-
590 3179.
- 591 41. Liu D, Xu H, Shih C, *et al.* T-B-cell entanglement and ICOSL-driven feed-forward regulation of
592 germinal centre reaction. *Nature* 2015; **517**: 214-218.
- 593 42. Reinhardt RL, Liang HE, Locksley RM. Cytokine-secreting follicular T cells shape the antibody
594 repertoire. *Nat Immunol* 2009; **10**: 385-393.
- 595 43. Weinstein JS, Hernandez SG, Craft J. T cells that promote B-Cell maturation in systemic
596 autoimmunity. *Immunol Rev* 2012; **247**: 160-171.
- 597 44. Siegemund S, Shepherd J, Xiao C, Sauer K. hCD2-iCre and Vav-iCre mediated gene
598 recombination patterns in murine hematopoietic cells. *PLoS One* 2015; **10**: e0124661.
- 599 45. Bolger AM, Lohse M, Usadel B. Trimmomatic: a flexible trimmer for Illumina sequence data.
600 *Bioinformatics* 2014; **30**: 2114-2120.
- 601 46. Dobin A, Davis CA, Schlesinger F, *et al.* STAR: ultrafast universal RNA-seq aligner. *Bioinformatics*
602 2013; **29**: 15-21.
- 603 47. Ritchie ME, Phipson B, Wu D, *et al.* limma powers differential expression analyses for RNA-
604 sequencing and microarray studies. *Nucleic Acids Res* 2015; **43**: e47.
605

606 **Figures**

607 Figure 1. **B cell phenotypes following hematopoietic cell-specific deletion of *Pou2af1*.**

608 **(a)** Percentage and **(b)** number of B cells in the spleen, PP and mLN of Vav-Cre⁻.*Pou2af1*^{fl/fl} and
609 Vav-Cre⁺.*Pou2af1*^{fl/fl} mice (n = 8, collected in six independent experiments). **(c)** Representative
610 flow cytometry profiles of GL-7 and FAS expression on total B cells gated as B220⁺ cells from
611 the mLN of Vav-Cre⁻.*Pou2af1*^{fl/fl} and Vav-Cre⁺.*Pou2af1*^{fl/fl} littermate controls. The gate selects
612 for GL-7⁺FAS⁺ GC B cells. **(d)** Percentage of GC B cells from the PP and mLN of Vav-Cre⁻
613 .*Pou2af1*^{fl/fl} and Vav-Cre⁺.*Pou2af1*^{fl/fl} littermate controls (n = 8, collected in six independent
614 experiments). **(e)** Representative flow cytometry profiles of CXCR4 and CD86 expression by GC
615 B cells from the mLN of Vav-Cre⁻.*Pou2af1*^{fl/fl} and Vav-Cre⁺.*Pou2af1*^{fl/fl} littermate controls. **(f)**
616 Ratio of dark zone (CXCR4^{Hi}CD86⁻) over light zone (CXCR4^{Low}CD86⁺) GC B cells from the PP
617 and mLN of Vav-Cre⁻.*Pou2af1*^{fl/fl} and Vav-Cre⁺ (n = 8, collected in six independent experiments).
618 Data information: Mann Whitney *U*-test, *P*-values * < 0.05; ** < 0.01; *** < 0.001.

619

620 Figure 2. ***Pou2af1* is expressed in activated T cells but does not affect T cell cytokine**
621 **production.**

622 **(a)** *Pou2af1* relative mRNA expression in spleen cells as well as in unactivated and activated T
623 cells from *Pou2af1*^{fl/fl} (Cre-), Vav-Cre⁺.*Pou2af1*^{fl/fl} (Vav-Cre+) and CD4-Cre⁺.*Pou2af1*^{fl/fl} (CD4-
624 Cre+) mice (n = 3-8, collected in three to four independent experiments), measured by RT-qPCR.
625 *Actb* was used as control. **(b)** Representative flow cytometry profiles of IL-2 expression by rested
626 and re-stimulated CD4⁺ T cells from the spleens of CD4-Cre⁻.*Pou2af1*^{fl/fl} and CD4-
627 Cre⁺.*Pou2af1*^{fl/fl} mice. **(c, d)** Percentage of IL-2-, TNF α - and IFN γ -producing CD4⁺ T cells after
628 re-stimulation of T cells from **(c)** CD4-Cre⁻.*Pou2af1*^{fl/fl} and CD4-Cre⁺.*Pou2af1*^{fl/fl} mice and **(d)**

629 *Vav-Cre⁻.Pou2af1^{fl/fl}* and *Vav-Cre⁺.Pou2af1^{fl/fl}* mice (n = 6, collected in three independent
630 experiments). **(e)** Percentage of IL-2-producing CD4⁺ T cells after re-stimulation of T cells from
631 *Vav-Cre⁻.Pou2af1^{fl/fl}* and *Vav-Cre⁺.Pou2af1^{fl/fl}* at the indicated anti-CD3 concentrations in the
632 presence of anti-CD28 (n = 3, collected in two independent experiments). **(f)** Representative flow
633 cytometry profiles of IL-2 expression by re-stimulated CD4⁺ T cells from *Vav-Cre⁻.Pou2af1^{fl/fl}* and
634 *Vav-Cre⁺.Pou2af1^{fl/fl}* mice, in absence of anti-CD28 antibodies. Representative of two
635 experiments. **(g)** Representative flow cytometry profiles of IL-2 expression by re-stimulated CD4⁺
636 T cells from the spleens of B6 and 129S mice. **(h)** IL-2 relative fluorescence intensity (RFI) of IL-
637 2-producing CD4⁺ T cells after re-stimulation of T cells from B6 and 129S mice (n = 6, collected
638 in three independent experiments). **(i)** IL-2 RFI of IL-2-producing CD4⁺ T cells after re-stimulation
639 of T cells from B6.129S-*Pou2af1^{-/-}* littermates carrying *Pou2af1* +/+, +/- and -/- genotypes (n =
640 6, collected in three independent experiments). NS, non-significant, *P*-value > 0.05, ***, *P*-value
641 < 0.001.

642

643 **Figure 3. *Pou2af1* does not affect Th17 differentiation and CD4⁺ T cell memory phenotype.**

644 **(a)** Representative flow cytometry profiles of RORγt expression by CD4⁺ T cells from the spleen
645 of *Vav-Cre⁻.Pou2af1^{fl/fl}* and *Vav-Cre⁺.Pou2af1^{fl/fl}* mice under Th0 and Th17 differentiation
646 conditions. MFI are indicated for each population. **(b)** IL-17A concentration in the supernatants
647 of T cell cultures from *Vav-Cre⁻.Pou2af1^{fl/fl}* and *Vav-Cre⁺.Pou2af1^{fl/fl}* mice under Th0 and Th17
648 differentiation conditions, measured by ELISA (n = 3, collected in three independent
649 experiments). **(c)** Representative flow cytometry profiles of IL-2 and IL-17A expression by CD4⁺
650 T cells from *Vav-Cre⁻.Pou2af1^{fl/fl}* and *Vav-Cre⁺.Pou2af1^{fl/fl}* mice under Th0 and Th17
651 differentiation conditions. **(d)** Representative flow cytometry profiles of RORγt expression by

652 CD4⁺ T cells from *Pou2af1*^{-/-} mice and control littermates under Th0 and Th17 differentiation
653 conditions. MFI of RORγt are indicated for each population. **(e)** Representative flow cytometry
654 profiles of IL-2 and IL-17A expression by CD4⁺ T cells from the same mice as in **(d)** under Th17
655 differentiation conditions. **(f, g)** Percentage (left panels) and absolute numbers (right panels) of
656 CD62L⁻CD44^{Hi}CD45RB⁻CD25⁻ CD4⁺ T cells from the spleen, bone marrow (BM) and of pool of
657 axial, brachial and inguinal LN of **(f)** *Vav-Cre*⁻.*Pou2af1*^{fl/fl} and *Vav-Cre*⁺.*Pou2af1*^{fl/fl} mice and **(g)**
658 *CD4-Cre*⁻.*Pou2af1*^{fl/fl} and *CD4-Cre*⁺.*Pou2af1*^{fl/fl} mice (n = 6, collected in three independent
659 experiments). Data information: Mann Whitney U-test, NS, non-significant, P-value > 0.05.

660

661 **Figure 4. OCA-B expression in non-T cells is necessary for Tfh maturation. (a)**
662 Representative flow cytometry profiles of CXCR5 and PD-1 expression on CD4⁺ T cells from the
663 PP of *Vav-Cre*⁻.*Pou2af1*^{fl/fl} and *Vav-Cre*⁺.*Pou2af1*^{fl/fl} mice. **(b, c)** Percentage of Tfh (CXCR5^{Hi}PD-
664 1^{Hi}) and early Tfh (CXCR5^{Low}PD-1^{Low}) in the PP of *Vav-Cre*⁻.*Pou2af1*^{fl/fl} and *Vav-Cre*⁺.*Pou2af1*^{fl/fl}
665 mice (n = 8, collected in three independent experiments). **(d)** PD-1 and CXCR5 relative
666 fluorescence intensity (RFI) on CXCR5⁺PD-1⁺ CD4⁺ T cells from the PP of *Vav-Cre*⁻.*Pou2af1*^{fl/fl}
667 and *Vav-Cre*⁺.*Pou2af1*^{fl/fl} mice (n = 8, collected in three independent experiments). **(e)**
668 Representative flow cytometry profiles of CXCR5 and PD-1 expression on CD4⁺ T cells from the
669 PP of *CD4-Cre*⁻.*Pou2af1*^{fl/fl} and *CD4-Cre*⁺.*Pou2af1*^{fl/fl} mice. **(f, g)** Percentage of Tfh and early
670 Tfh in the PP of *CD4-Cre*⁻.*Pou2af1*^{fl/fl} and *CD4-Cre*⁺.*Pou2af1*^{fl/fl} mice (n = 10, collected in three
671 independent experiments). **(h)** Percentage of GC B cells in the PP of *CD4-Cre*⁻.*Pou2af1*^{fl/fl} and
672 *CD4-Cre*⁺.*Pou2af1*^{fl/fl} mice (n = 10, collected in three independent experiments). **(i)** Ratio of dark
673 zone (CXCR4^{Hi}CD86⁻) over light zone (CXCR4^{Low}CD86⁺) GC B cells from the PP of *CD4-Cre*⁻
674 *.Pou2af1*^{fl/fl} and *CD4-Cre*⁺.*Pou2af1*^{fl/fl} mice (n = 10, collected in three independent experiments).

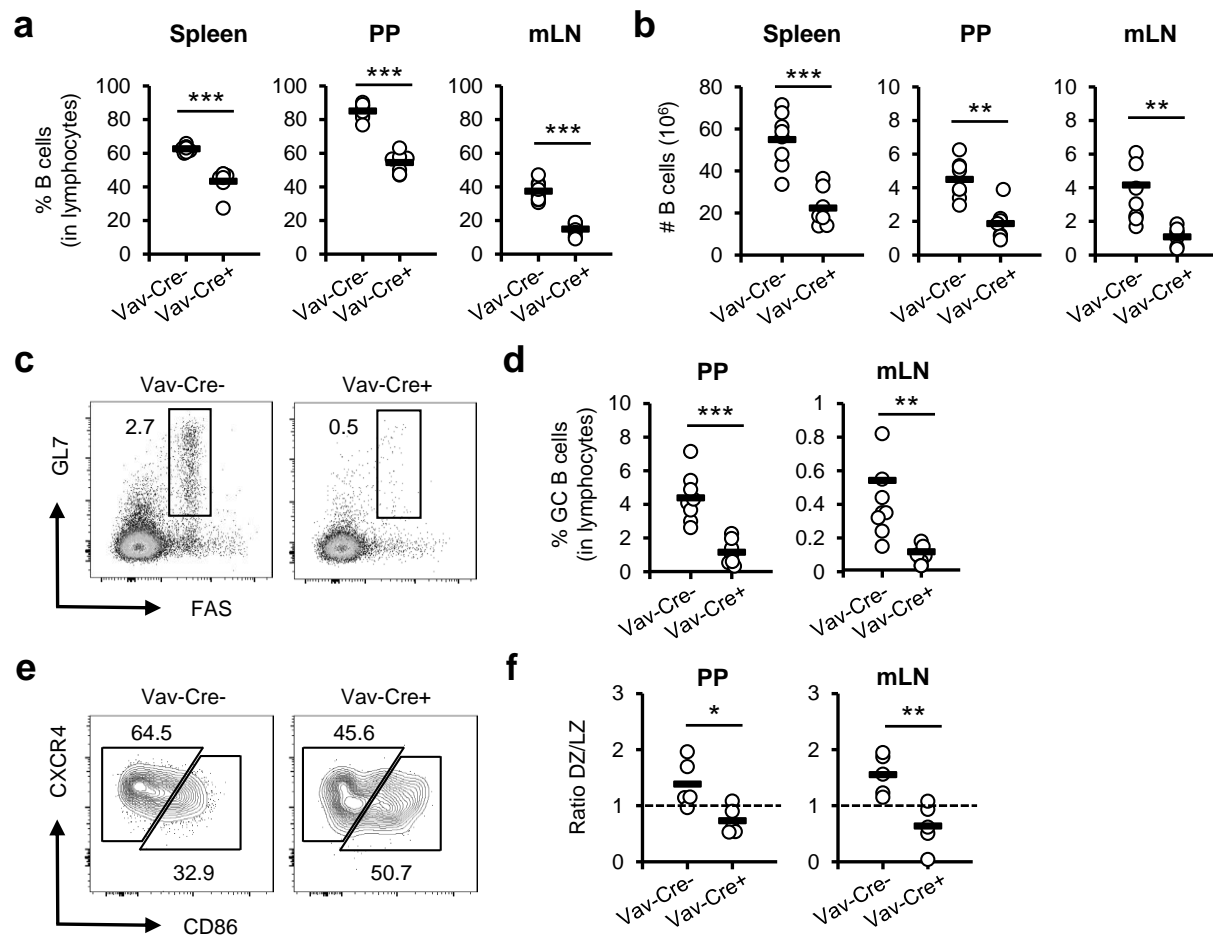
675 **(j)** Representative flow cytometry profiles of Tfh (CXCR5^{Hi}PD-1^{Hi}) from the spleen of immunized
676 Cre⁻.*Pou2af1*^{fl/fl}, Vav-Cre⁺.*Pou2af1*^{fl/fl} and CD4-Cre⁺.*Pou2af1*^{fl/fl} mice. **(k)** Percentage of Tfh cells
677 in the spleen of the same groups of mice listed in **(j)** (n > 5, collected in four independent
678 experiments). **(l)** Percentage of GL-7⁺FAS⁺ GC B cells in the spleen, assessed by flow
679 cytometry, of the same groups of mice listed in **(j)** (n > 5, collected in four independent
680 experiments). Data information: Mann Whitney *U*-test for figures **(b-d, f-i)**. One-way ANOVA for
681 figures **(k-l)**, NS, non-significant *P*-value > 0.05; *P*-values ** < 0.01; *** < 0.001.

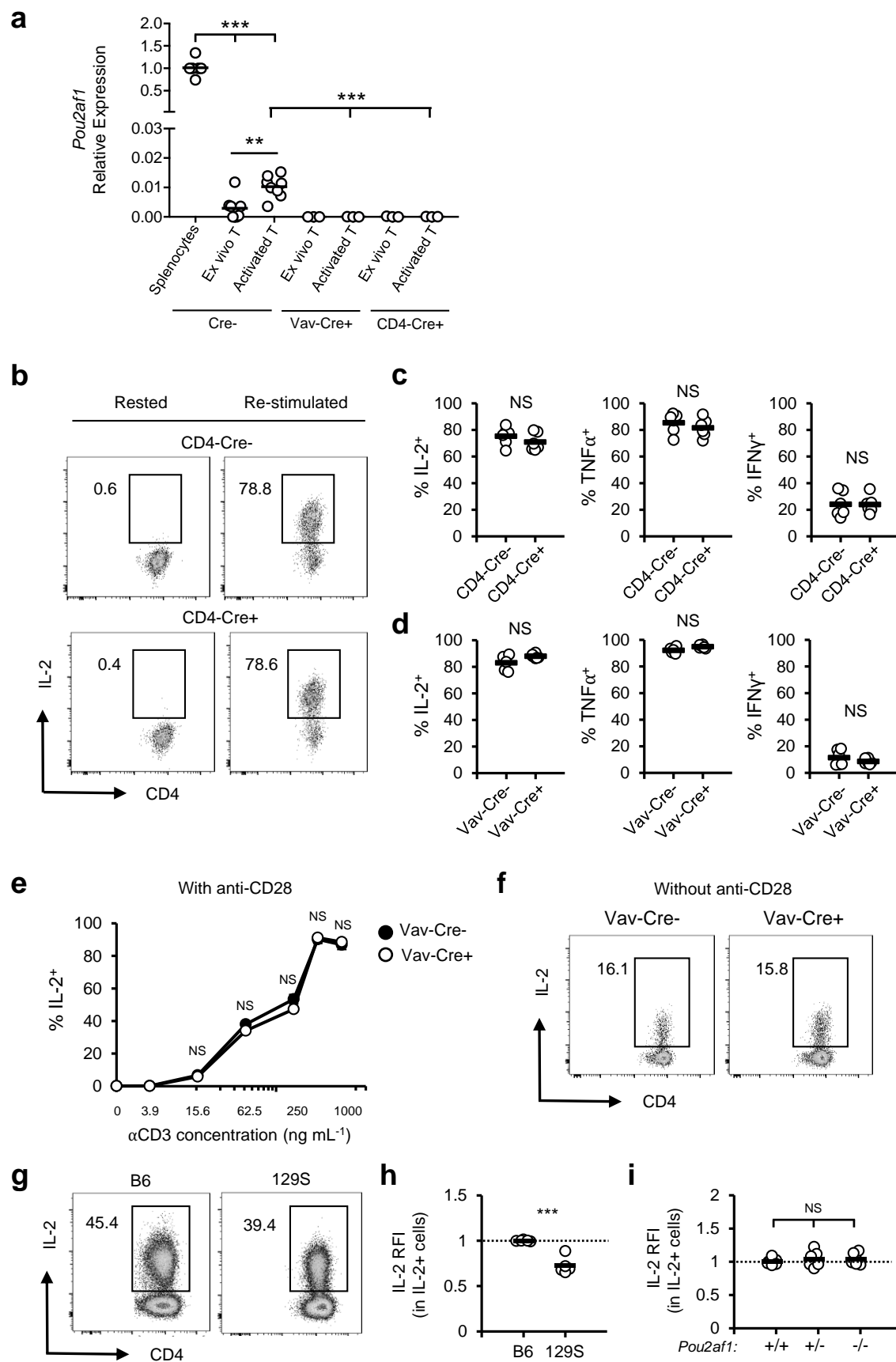
682

683 **Figure 5. OCA-B is not an active transcriptional coactivator in CD4⁺ and CD8⁺ T cells and**
684 **is required in B cells to facilitate Tfh differentiation.**

685 **(a)** Principal Component Analysis of top 500 most variable genes from CD4⁺ and CD8⁺ T cell
686 RNA-Seq samples from the spleen of CD4-Cre⁻.*Pou2af1*^{fl/fl} (WT), CD4-Cre⁺.*Pou2af1*^{fl/+} (Het) and
687 CD4-Cre⁺.*Pou2af1*^{fl/fl} (KO) mice. **(b)** Row-normalized (z-score) expression heatmap of selected
688 DEGs, where each row represents a gene and columns represent individual samples. Red
689 represents a higher relative expression for a given gene, while blue denotes a lower relative
690 expression. Column annotation tracks represent sample cell type and genotype. **(c)**
691 Representative flow cytometry profiles of CD45.1 and CD45.2 expression on B (left panel) and
692 T (right panel) cells from the spleen of the chimeras. **(d)** Ratio of CD45.1⁺ (WT genotype) over
693 CD45.2⁺ (KO genotype) cells in the spleen of the chimeras (n = 5, collected in two independent
694 experiments). **(e)** Representative flow cytometry profiles of Tfh from the PP of Vav-Cre⁻
695 *.Pou2af1*^{fl/fl}, Vav-Cre⁺.*Pou2af1*^{fl/fl} and the bone marrow competitive chimeras, for which the
696 profiles are separated based on CD45.1⁺ and CD45.2⁺ expression. **(f)** Percentage of Tfh in the
697 spleen, PP and mLN of the chimeras, gated based on the expression of CD45.1 (B6.SJL) and

698 CD45.2 (*Vav-Cre⁺.Pou2af1^{fl/fl}*) to identify the origin and, thus the genotype, of the donor cells (n
699 = 5, collected in two independent experiments). **(g)** Percentage of B cells in the PP and mLN of
700 CD19-Cre⁻.*Pou2af1^{fl/fl}* and CD19-Cre⁺.*Pou2af1^{fl/fl}* mice, **(h)** percentage of Tfh in the PP and mLN
701 of CD19-Cre⁻.*Pou2af1^{fl/fl}* and CD19-Cre⁺.*Pou2af1^{fl/fl}* mice, and **(i-j)** CXCR5 and PD-1 RFI on
702 CXCR5⁺PD-1⁺ CD4⁺ T cells from the PP of CD19-Cre⁻.*Pou2af1^{fl/fl}* and CD19-Cre⁺.*Pou2af1^{fl/fl}*
703 mice (n = 7-10, collected in five independent experiments). Data information: Mann Whitney *U*-
704 test, NS, non-significant, *P*-value > 0.05; *P*-values ** < 0.01; *** < 0.001.





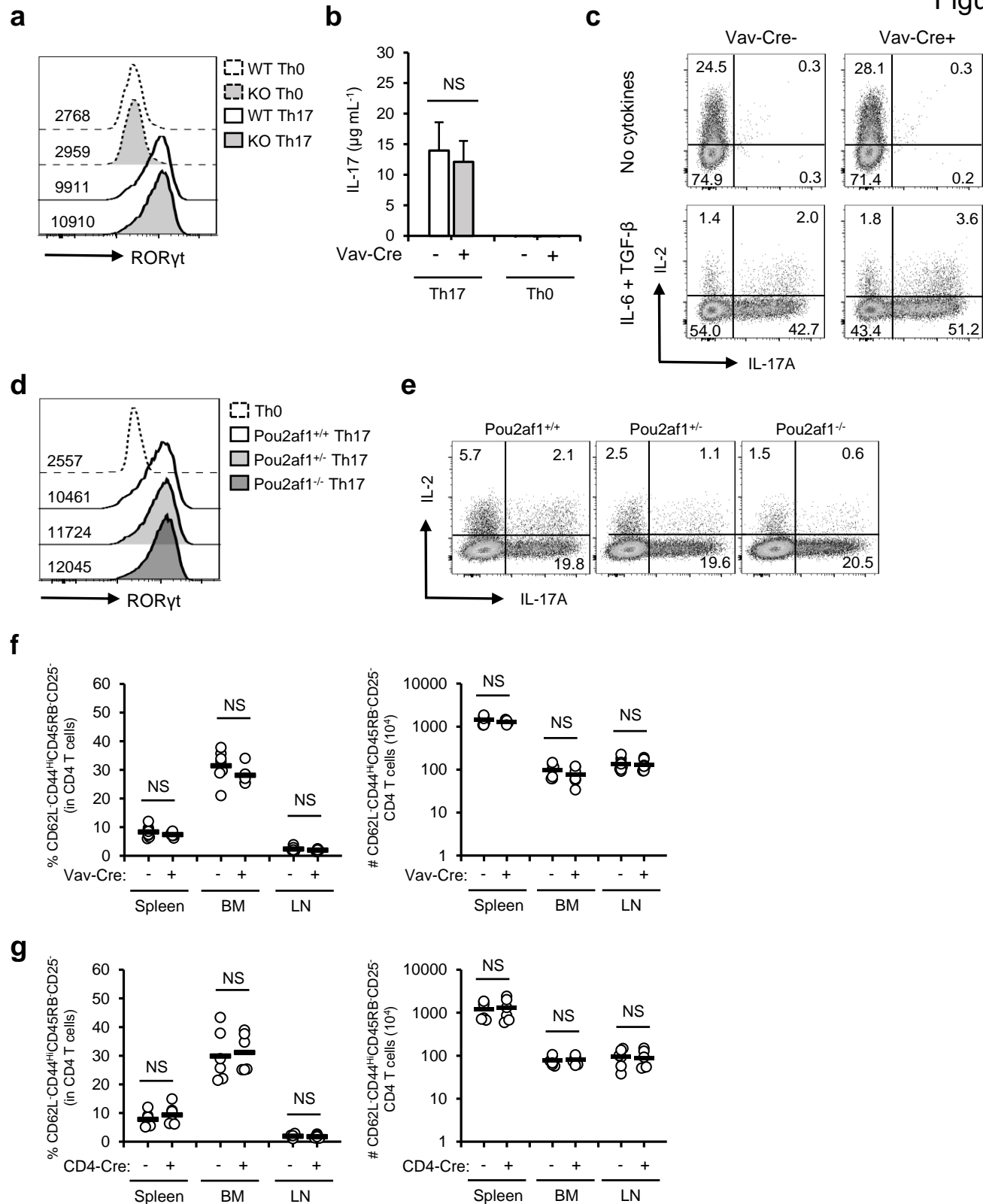
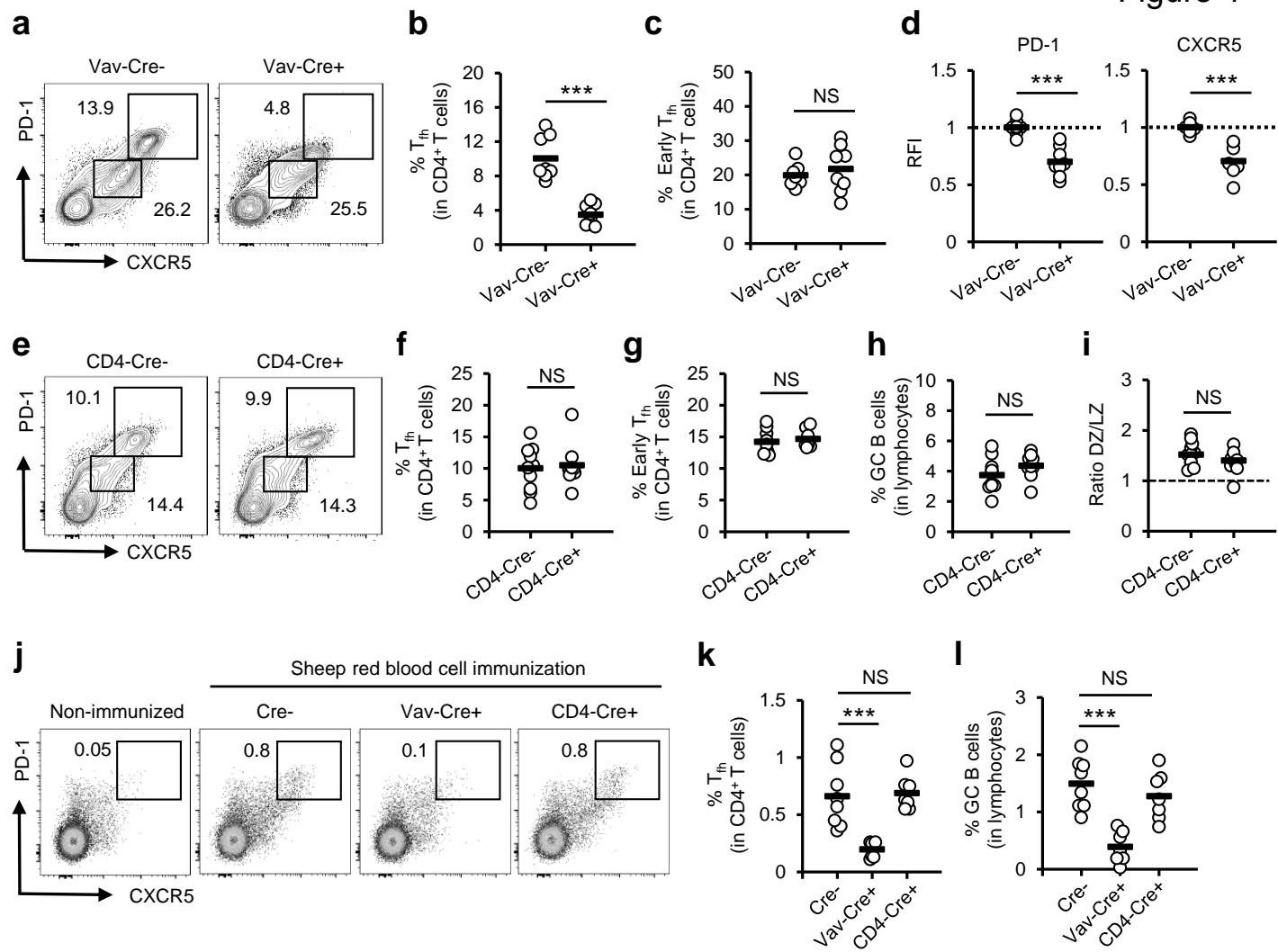
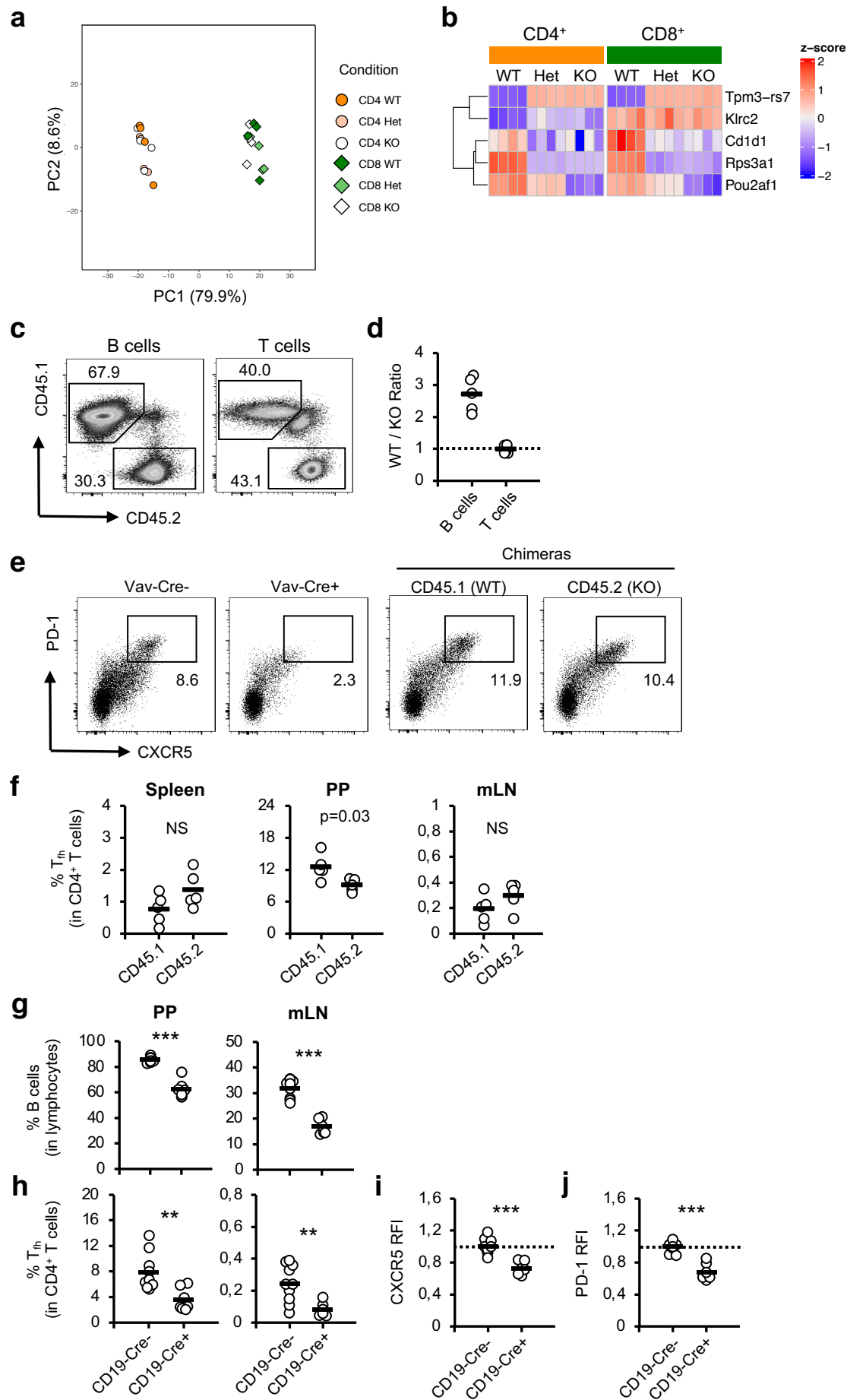
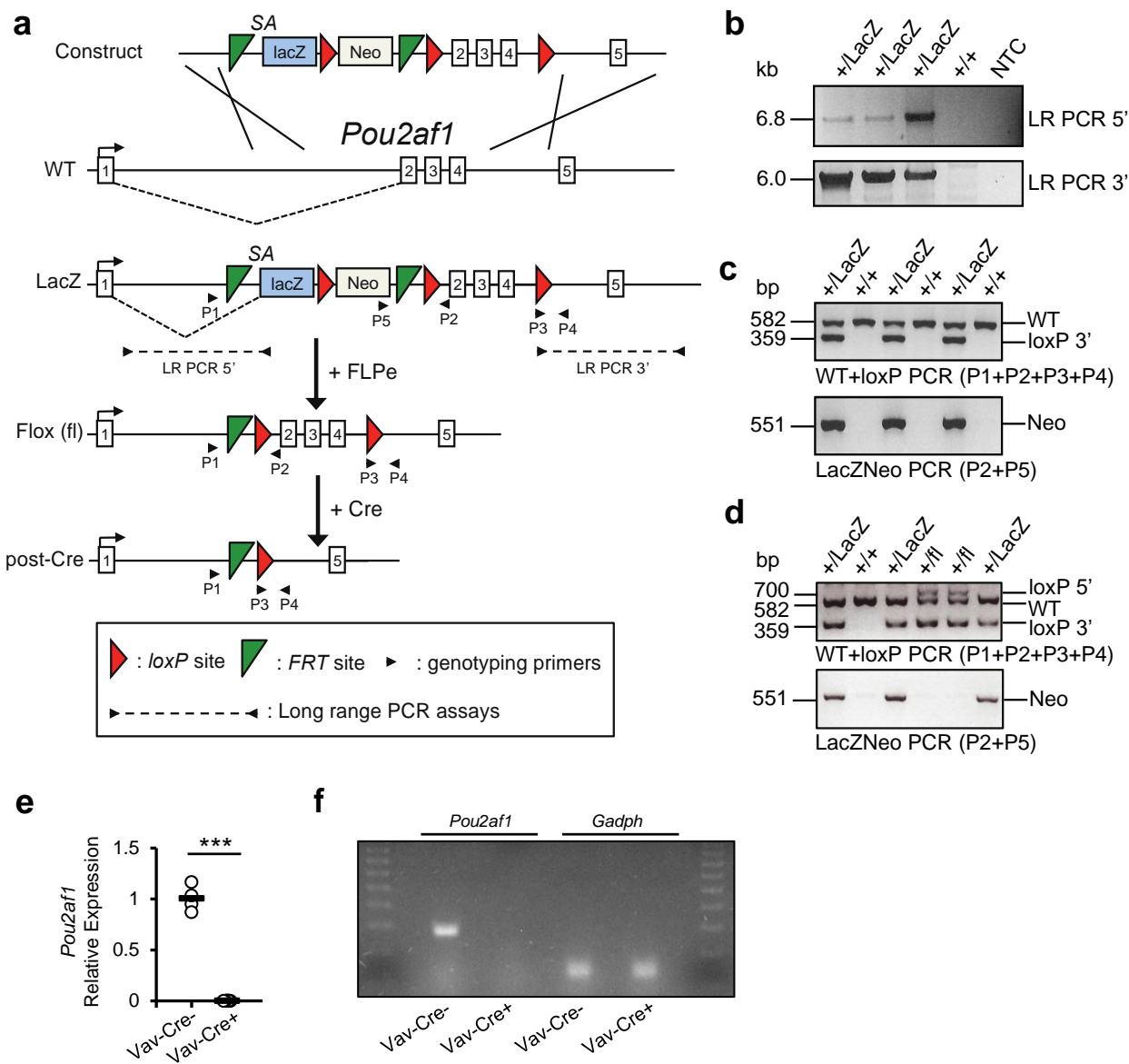


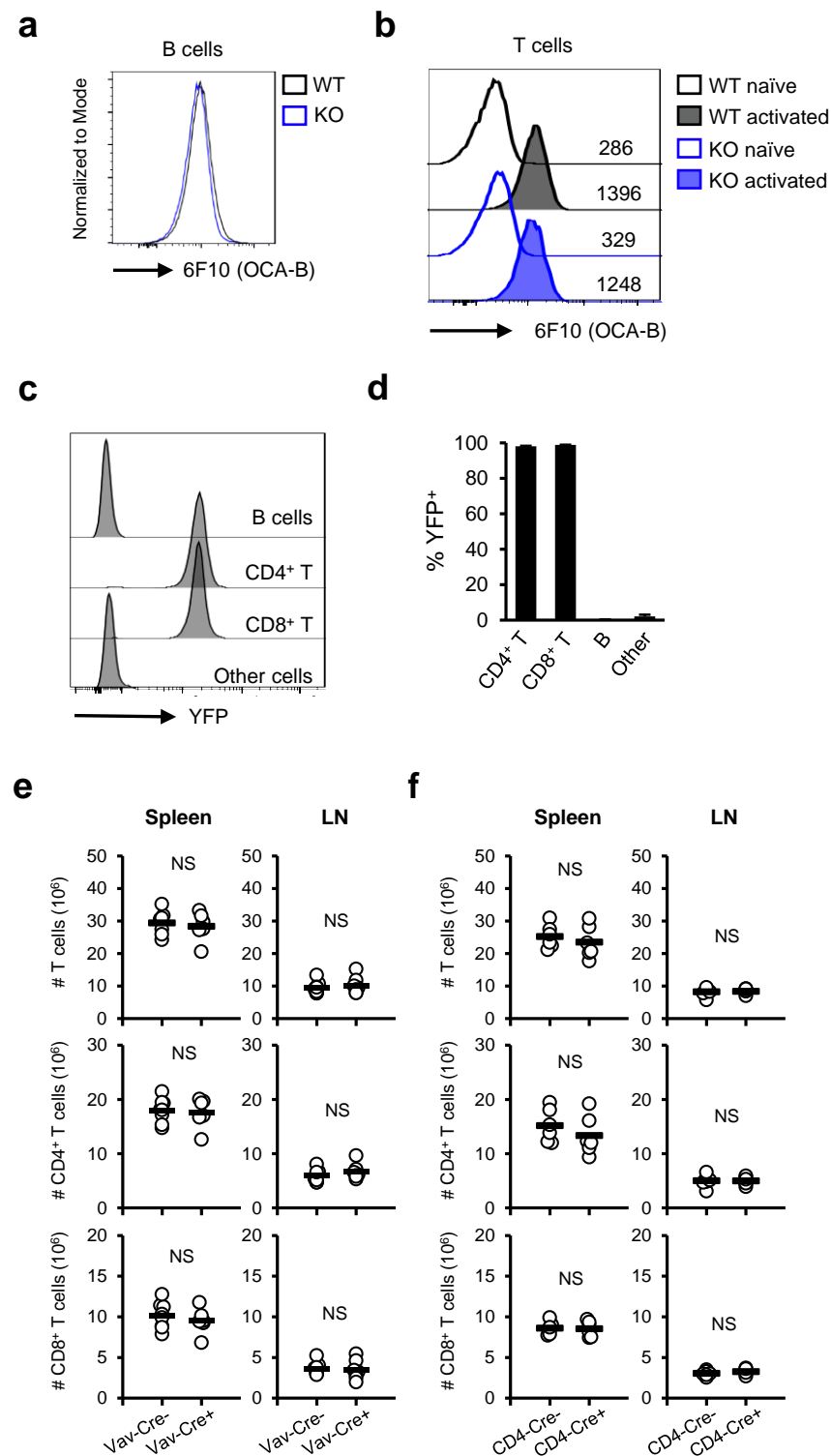
Figure 4



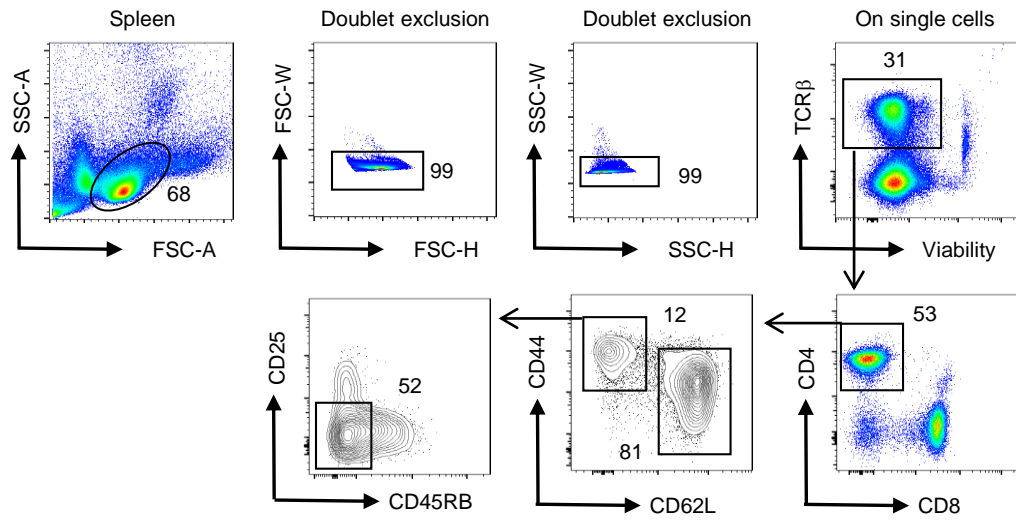




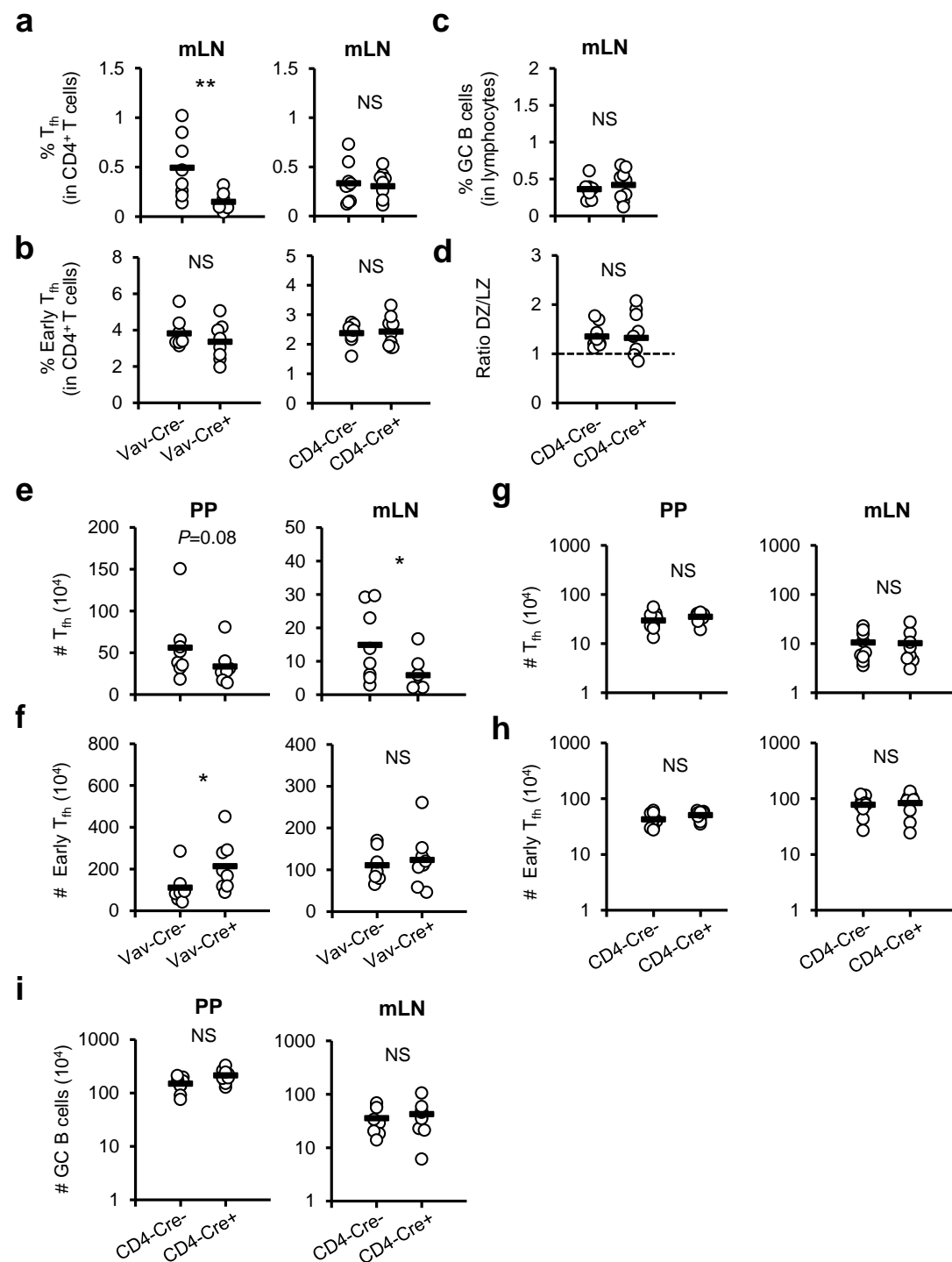
Supplementary figure 1. **Generation of a *Pou2af1^{fl/fl}* mouse for cell specific deletion of *Pou2af1*.** (a) Targeting strategy used to generate *Pou2af1^{+LacZ}* and *Pou2af1^{+/fl}* mice. The position of the primers and long-range PCR assays used for genotyping are indicated. SA: splice acceptor site located in front of the lacZ cassette. (b) Long range PCR on mouse tail DNA confirming the proper targeting of the *Pou2af1* locus. (c) Genotyping PCR demonstrating the generation of *Pou2af1^{+LacZ}* mice. (d) Genotyping PCR demonstrating the generation of *Pou2af1^{+/fl}* mice following breeding with *ACTBFLPe* mice. (e) *Pou2af1* relative expression in splenocytes from *Vav-Cre⁻.Pou2af1^{fl/fl}* and *Vav-Cre⁺.Pou2af1^{fl/fl}* mice ($n = 4$, collected in two independent experiments), measured by RT-qPCR. *Gadph* mRNA levels were used as loading control. (f) *Pou2af1* and *Gadph* RT-qPCR products were migrated on agarose gel for mice of the indicated genotypes. ***, P -value < 0.001 .



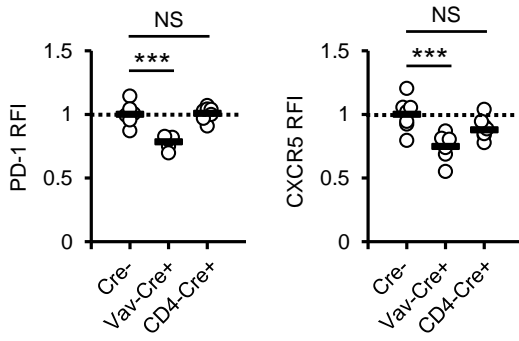
Supplementary figure 2. **Validation of tools to the study of OCA-B expression and function in T cells.** **(a)** Representative flow cytometry profiles of 6F10 staining on B cells from Vav-Cre⁻.*Pou2af1*^{fl/fl} and Vav-Cre⁺.*Pou2af1*^{fl/fl} mice. **(b)** Representative flow cytometry profiles of 6F10 staining on naïve and activated T cells from Vav-Cre⁻.*Pou2af1*^{fl/fl} and Vav-Cre⁺.*Pou2af1*^{fl/fl} mice. MFI are indicated for each population. **(c)** Representative flow cytometry profiles of YFP expression on cells from the spleen of CD4-Cre⁺.ROSA-YFP⁺ mice. **(d)** Percentage of YFP⁺ cells from the spleen of CD4-Cre⁺.ROSA-YFP⁺ mice (n = 3, collected in one experiment). **(e)** Numbers of total, CD4⁺ and CD8⁺ T cells from the spleen and a pool of inguinal, axillary and brachial LN of Vav-Cre⁻.*Pou2af1*^{fl/fl} and Vav-Cre⁺.*Pou2af1*^{fl/fl} mice (n = 6, collected in three independent experiments), and **(f)** CD4-Cre⁻.*Pou2af1*^{fl/fl} and CD4-Cre⁺.*Pou2af1*^{fl/fl} mice (n = 6, collected in three independent experiments). NS, non-significant, P-value > 0.05



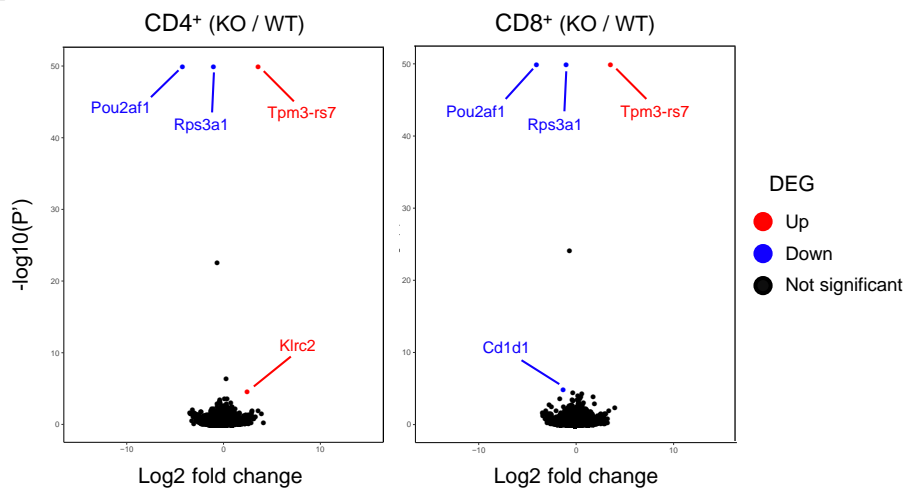
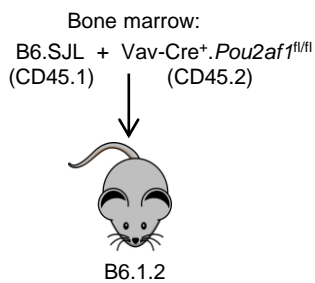
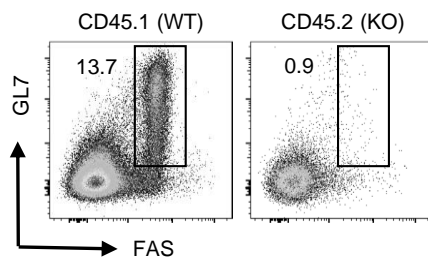
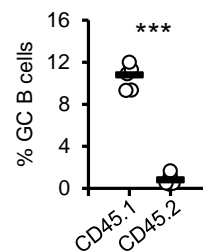
Supplementary figure 3. **Gating strategy for the analysis of CD4⁺ T cells with a memory phenotype.** Representative flow cytometry profiles of cells from the spleen of *Vav-Cre; Pou2af1^{fl/fl}* mice.



Supplementary figure 4. **Hematopoietic cell-specific but not T cell-specific *Pou2af1* deletion limits Tfh maturation.** (a, b) Percentage of (a) Tfh (CXCR5^{Hi}PD-1^{Hi}) and (b) early Tfh (CXCR5^{Low}PD-1^{Low}) in the mLN of Vav-Cre⁻.*Pou2af1*^{fl/fl}, Vav-Cre⁺.*Pou2af1*^{fl/fl} mice, CD4-Cre⁻.*Pou2af1*^{fl/fl} and CD4-Cre⁺.*Pou2af1*^{fl/fl} mice (n = 8-10, collected in three independent experiments). (c) Percentage of GC B cells in the mLN of CD4-Cre⁻.*Pou2af1*^{fl/fl} and CD4-Cre⁺.*Pou2af1*^{fl/fl} mice (n = 10, collected in three independent experiments). (d) Ratio of dark zone (CXCR4^{Hi}CD86⁻) over light zone (CXCR4^{Low}CD86⁺) GC B cells from the mLN of CD4-Cre⁻.*Pou2af1*^{fl/fl} and CD4-Cre⁺.*Pou2af1*^{fl/fl} mice (n = 10, collected in three independent experiments). (e-h) Absolute numbers of Tfh and early Tfh cells from the PP and mLN of (e, f) Vav-Cre⁻.*Pou2af1*^{fl/fl} and Vav-Cre⁺.*Pou2af1*^{fl/fl}, and (g, h) of CD4-Cre⁻.*Pou2af1*^{fl/fl} and CD4-Cre⁺.*Pou2af1*^{fl/fl} mice (n = 10, collected in three independent experiments). (i) Absolute numbers of GC B cells from the PP and mLN of CD4-Cre⁻.*Pou2af1*^{fl/fl} and CD4-Cre⁺.*Pou2af1*^{fl/fl} mice (n = 10, collected in three independent experiments). NS, non-significant, *P*-value > 0.05; *P*-values * < 0.05, ** < 0.01.

a

Supplementary figure 5. ***Pou2af1* deletion impacts Tfh maturation and GC formation in a T cell-extrinsic manner.** (a) PD-1 and CXCR5 RFI on CXCR5⁺PD-1⁺ CD4⁺ T cells from the spleen of the same groups of mice listed in Figure 4j, namely sheep red blood cell immunized Cre⁻.*Pou2af1*^{fl/fl}, Vav-Cre⁺.*Pou2af1*^{fl/fl} and CD4-Cre⁺.*Pou2af1*^{fl/fl} mice (n = 6-8, collected in four independent experiments). NS, non-significant, *P*-value > 0.05; ***, *P*-value < 0.001.

a**b****c****d**

Supplementary figure 6. **OCA-B is not an active transcriptional coactivator in CD4⁺ and CD8⁺ T cells.**

(a) Volcano Plots of Differentially Expressed Genes (DEG) from CD4⁺ (left) and CD8⁺ (right) T cells of CD4-Cre⁺.*Pou2af1*^{fl/fl} and CD4-Cre⁺.*Pou2af1*^{fl/fl} mice at FDR <0.05 and Fold Change > 1.5. Genes upregulated in the KO are in red, downregulated in blue, and black if not significantly differentially expressed. **(b)** Schematic representation of the competitive bone marrow chimeras. **(c)** Representative flow cytometry profiles of GL7⁺FAS⁺ GC cells in B220⁺ B cells from the PP of the chimeras. **(d)** Percentage of GC B cells in the PP of the chimeras (n = 5, collected in two independent experiments). ***, P < 0.001.